WIRELESS PHYSICAL LAYER NETWORK CODING FOR MULTIPLE ANTENNA SYSTEMS

A Thesis Submitted to
the Graduate School of
İzmir Institute of Technology
in Partial Fulfillment of the Requirements for the Degree of

MASTER OF SCIENCE

in Electronics and Communication Engineering

by
Mert İLGÜY

December 2020
İZMİR

ACKNOWLEDGMENTS

First of all, I would like to thank to my supervisor Assoc. Dr. Prof. Berna Özbek who has always helped me and shared her knowledge during my preparation of this thesis. In addition, I present my respect and love to my dear mother Çiğdem Çağlayan İlgüy and my dear father Kahraman İlgüy, who have demonstrated all their material and spiritual support for me since the day I was born. Moreover, I present my deepest gratitude to my very dear grandmother, Zişan İlgüy, who is not with us at the moment. She has fostered me when I was a child while my mother and father were working. She had always dreamed for me having a very good occupation and being in good places all the time in the rest of my life.

Finally, in academic life, I thank to dear Mustafa Can Güden, Olgu Erten, Niyazi Toker, Fikrican Pusat, Nuri Koyuncu, Kerem Maden, Burhan Sünbül, Burak Öztürk and Oğulcan Erdoğan. They worked with me on the most difficult days of undergraduate and graduate studies. I owe some of my achievements. I convey my deepest love to them.

ABSTRACT

WIRELESS PHYSICAL LAYER NETWORK CODING FOR MULTIPLE ANTENNA SYSTEMS

Wireless networks are prone to interference due to their broadcast nature. In the design of most of the traditional networks, this broadcast nature is perceived as a performance-degrading factor. However, physical layer network coding (PNC) exploits this broadcast nature by enabling simultaneous transmissions from different sources and facilitates an increase in the spectral efficiency of the wireless networks. Besides, the massive multiple input multiple output (MIMO) is considered as one of key technologies to improve the spectral efficiency for wireless communication systems. The combination of PNC and multi-user massive MIMO in the sixth generation (6G) networks can increase further the spectral efficiency.

In this thesis, PNC based systems are examined via bit error rate (BER) and coverage probability by focusing on the BER of the network coded symbol (NCS). Hence, PNC based systems are compared with network coding (NC) and conventional schemes. The influence of the signal-to-noise ratio (SNR) differences of the users are examined on the BER performances. Thereby, an alternative method to estimate NCS is proposed for the MIMO-PNC systems without using log likelihood ratio (LLR). We derive a closed form expression for the coverage probability in PNC based multi-user massive MIMO systems by employing zero forcing (ZF) equalization. The non-orthogonal multiple access (NOMA) based PNC system is proposed. We show the applicability of the PNC in the NOMA based MIMO systems by giving the the BER performance results.

ÖZET

ÇOKLU ANTEN SİTEMLERİ İÇİN KABLOSUZ FİZİKSEL KATMAN AĞI KODLAMASI

Kablosuz ağlar, yayın yapıları nedeniyle girişime eğilimlidir. Geleneksel ağların çoğunun tasarımında, bu yayın doğası performansı düşüren bir faktör olarak algılanmaktadır. Bununla birlikte, fiziksel katman ağ kodlaması, farklı kaynakların eş zamanlı iletimlerini mümkün kılarak bu yayın niteliğini kullanır ve kablosuz ağların spektral verimliliğindeki artışı kolaylaştırır. Ayrıca, masif çoklu giriş çoklu çıkış, kablosuz iletişim sistemleri için spektral verimliliği arttıran anahtar teknolojilerden biri olarak kabul edilir. Altıncı nesil (6G) ağlarda fiziksel katman ağ kodlaması ve çok kullanıcılı masif çoklu giriş çoklu çıkış kombinasyonu, spektral verimliliği daha da arttırabilir.

Bu tezde, fiziksel katman ağ kodlaması bit hata oranı ve kapsama olasılığı baz alınarak incelenmiştir. Tez boyunca, ağ kodlu sembolün bit hata oranına odaklanılmıştır. Fiziksel katman ağ kodlaması, ağ kodlaması ve geleneksel iletim ile karşılaştırılır. Kullanıcıların sinyal-gürültü oranları farklılıklarının bit hata oranı performansları üzerindeki etkisi incelenmiştir. Ayrıca, ağ kodlu sembolünü tahmin etmek için logaritmik olabilirlik oranı kullanılmayan alternatif bir yöntem, çoklu giriş çoklu çıktılı fiziksel katman ağ kodlaması sistemleri için önerilmektedir. Fiziksel katman ağı tabanlı çok kullanıcılı masif çoklu giriş çoklu çıkışlı sistemlerde kapsama olasılığının sıfır zorlamalı eşitleme kullanarak kapalı form ifadesi türetilmektedir. Dikgen olmayan çoklu erişim tabanlı bir fiziksel katman ağı sistemi önerilmektedir. Performans sonucu olarak bit hata oranı verilerek dikgen olmayan çoklu erişim tabanlı çoklu giriş çoklu çıkış sistemlerinde fiziksel katman ağı kodlamasının uygulanabilirliğini gösterilmektedir.

TABLE OF CONTENTS

LIST OF FIGURES

Figure **Page**

Figure **Page**

LIST OF TABLES

Table **Page**

LIST OF ABBREVIATIONS

AWGN . . . . . Additive White Gaussian Noise
B5G . . . . . Beyond Fifth Generation
BC . . . . . Broadcast Channel
BER . . . . . Bit Error Rate
BPSK . . . . . Binary Phase Shift Keying
BS . . . . . Base Station
CCDF . . . . . Complementary Cumulative Distribution function
CDF . . . . . Cumulative Distribution Function
CSI . . . . . Channel State Information
EM . . . . . Electromagnetic
HI . . . . . Hierarchical Information
HSI . . . . . Hierarchical Side Information
IoT . . . . . Internet of Things
LLR . . . . . Log Likelihood Ratio
LR . . . . . Likelihood Ratio
M-PSK . . . . . M-ary Phase Shift Keying
M-QAM . . . . . M-ary Quadrature Amplitude Modulation
MAC . . . . . Multiple Acces Channel
MIMO . . . . . Multiple Input Multiple Output
MIMO-NC . . . . . Multiple Input Multiple Output Network Coding
MIMO-PNC . . . . . Multiple Input Multiple Output Physical Layer Network Coding
MMSE . . . . . Minimum Mean Squared Error
NOMA . . . . . Non-Orthogonal Multiple Access
NC . . . . . Network Coding
NCS . . . . . Network Coded Symbol
OMA . . . . . Orthogonal Multiple Access
PDF . . . . . Probability Density Function
PSD . . . . . Power Spectral Density
PNC . . . . . Physical Layer Network Coding
QoS . . . . . Quality of Service

QPSK . . . . . Quadrature Phase Shift Keying

SISO . . . . . Single Input Single Output

SIC . . . . . Successive Interference Cancellation

SNR . . . . . Signal to Noise Ratio

SIMO-PNC . . . . . Single Input Multiple Output Physical Layer Network Coding

UE . . . . . User Equipment

V-BLAST . . . . . Vertical Bell Labs Space Time

XOR . . . . . Exclusive-OR

ZF . . . . . Zero Forcing

3G . . . . . Third Generation

6G . . . . . Sixth Generation

CHAPTER 1

INTRODUCTION

The interference is seemed to be one of the biggest difficult situation when the linear combination of the signals coming from different sources occurs. The data is transmitted via electromagnetic (EM) waves in the radio channel of the physical layer of the wireless networks. The interference between these waves results in errors in the transmission of the data. Most of the traditional network design is addressed to decrease interference with transmission scheduling or receiver design. In (Zhang and Liew, 2010), the interference is seemed to be situation that must be embraced to improve the network capacity. In order to make this improvement real the authors give some objectives which must be met. A relay can transform the simultaneously received signal to an output form which can be interpreted in the final destination. A destination must be able to extract the information directed to it from relayed signal.

MIMO has been the key technology since the emergence of third generation (3G). The main objective of the MIMO is to increase the spectral efficiency, the range and/or link reliability by using multiple antennas in the transmitter and receiver. However, since the multiple signals transmitted and received through multiple antennas, they face with the interference. Thus, a need occurs to detect these multiple signals in the receiver correctly. In the literature, the interest in the MIMO detector has preserved its continuity for the past fifty years. The detection of the multiple signals in MIMO system has been hold separately or jointly. Joint detection is able to reach a significant better performance rather than the separate detection with a high computational complexity. MIMO detection can be mainly classified as linear MIMO detection and interference-cancellation based MIMO detection etc. The linear MIMO detection techniques can be classified into sub-optimum techniques which are ZF and minimum mean squared error (MMSE) detection.

In (Albreem et al., 2019), the authors state that massive MIMO is seemed to be a key technology to encounter the user demands and increase the quality of service (QoS) for the current wireless systems. Massive MIMO systems are the natural extension of the MIMO systems. A base station (BS) in the massive MIMO system can serve a large

number of users equipped with single or few antennas in the same frequency band. In the massive MIMO systems, the number of the antennas used in BS is higher than the user equipment (UE) in the cell or the service area. Then, in (Okyere et al., 2019), PNC based systems are considered in the massive MIMO systems.

NOMA is one of the significant radio access techniques for performance improvement in next-generation cellular communications. NOMA provides a higher spectrum efficiency compared with the orthogonal frequency division multiple access which is a well-known high-capacity orthogonal multiple access (OMA) technique. The main types of NOMA techniques can be classified as power-domain NOMA and code-domain NOMA (Islam et al., 2017). The combination of NOMA and PNC has been held in (Ho and Leow, 2019) without considering MIMO.

The aim of this thesis is to examine the performance of PNC based on BER and coverage probability in single antenna systems, MIMO systems, massive MIMO systems and NOMA systems. The thesis is organized as follows:

- In Chapter 2, we give the theoretical background of PNC for single input single output (SISO) systems and multi-user massive MIMO systems. We explain the main transmission schemes in the two-way relay networks. We compare the BER performance of the PNC and the other schemes. We consider the SNR difference between the users while the performance results are held. We give a low complex method to estimate NCS without using LLR.

- In Chapter 3, we analyze the coverage probability of PNC. We give the related works which focus the coverage probability of the MIMO systems with and without PNC. We define the SNR value after equalization for PNC. We derive a closed form coverage probability expression for a user pair in a multi-user massive MIMO-PNC system. We give the theoretical and simulation results of the average coverage probability for different scenarios.

- In Chapter 4, we propose a NOMA based MIMO-PNC system. We present the related works in the literature. We define two pairing scenarios for NOMA based MIMO-PNC and give the algorithm to merge NOMA and MIMO-PNC. We give the BER performances for NOMA based MIMO-PNC.

- Chapter 5 concludes the thesis.

CHAPTER 2

PHYSICAL LAYER NETWORK CODING

In this chapter, background information about PNC based systems is given. Firstly, two-way relay channel is represented. Then, in this channel, three different data exchange methods are introduced. Next, PNC is examined for binary phase shift keying (BPSK) and quadrature phase shift keying (QPSK) modulations in Rayleigh fading channels. Hence, BER expressions for PNC, NC and conventional transmission are derived. Then, PNC for multi-user massive MIMO systems are examined. Finally, the performance evaluations are given for different cases.

2.1. Two-Way Relay Channel

Two-way relay channel has been originated from Shannon's work which is two-way channel consisting two terminal nodes (N_1, N_2) which want to exchange their data simultaneously. For this scenario, the signals which are transmitted from two terminal nodes interfere each other. When the nodes are far away from each other, an intermediate node is needed to increase the coverage which is named as relay (R).

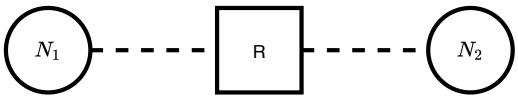

Figure 2.1. Two-way relay channel

The relay provides a lower power consumption by dividing total distance into small distances for node-to-node transmissions. Two-way relay channel given in Figure 2.1 can be seen as two-way channel with an additive intermediate relay node. Hence, the overall transmission is divided into two phases. The signal transmission from terminal nodes to the relay node is called multiple access channel (MAC) phase. On the other hand, the signal transmission from relay to terminal nodes is called broadcast channel

(BC) phase. As a minimalist scenario, for mobile communication, two terminal nodes can be considered as UEs. Then, the relay can be considered as BS. In this case, uplink corresponds to MAC phase and downlink is identical to BC phase. In the literature, there are three different approaches for the data exchange between two terminal nodes.

First approach divides the transmission into four time slots. In first time slot, first terminal node sends its data to the relay and in the second time slot, the relay just amplifies and forwards the coming data to the second terminal node. In third time slot, N_2 sends its data to the relay. After, in the fourth time slot, relay amplifies and forwards the data to the first terminal node. The conventional four time slot transmission is the first consideration about how the terminal nodes exchange their data. This scheme is given in Figure 2.2 which is not spectral efficient since the transmission needs four orthogonal time slots.

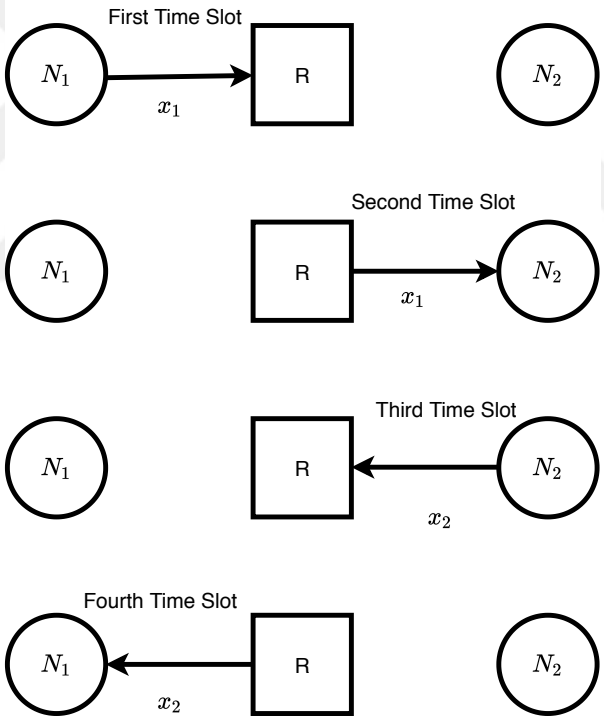

Figure 2.2. Conventional data transmission

In order to increase the spectral efficiency, NC can be used. For this approach, first terminal node sends its data to the relay. After, the relay detects and stores the bits coming from the first node. Then, in the second time slot, second terminal node sends its data to the relay and relay detects and stores the bits. In the third time slot, the relay operates exclusive-OR (XOR) operation of the stored bits and broadcasts them to the

terminal nodes. Since terminal nodes know their own data, they can extract the data of other node by operating XOR operation again. NC scheme is described in Figure 2.3.

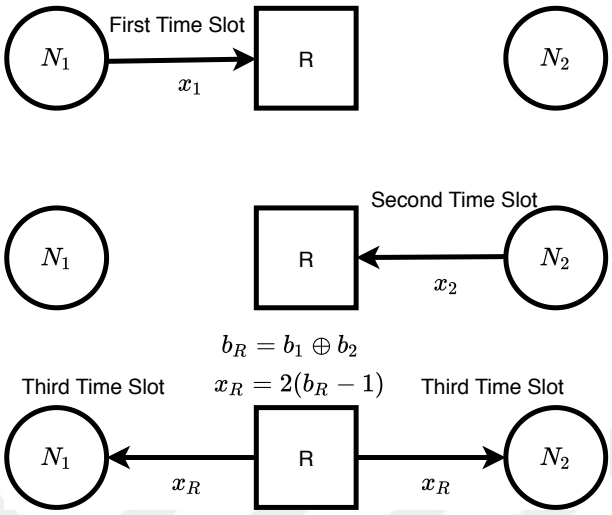

Figure 2.3. Data transmission with NC

The third approaches is called PNC. This scheme allows two simultaneous transmissions in the same time slot. Terminal nodes transmit their signals in the first time slot. After, the relay receives the combined signal and decides on the NCS. PNC maps directly the received constellation points to their corresponding NCSs without applying the bit-wise network coding operation while NC separately detects the terminal node's data in different time slots to perform their bit-wise network coding operation. For binary case, the optimal network coding operation is XOR. PNC scheme is represented in Figure 2.4.

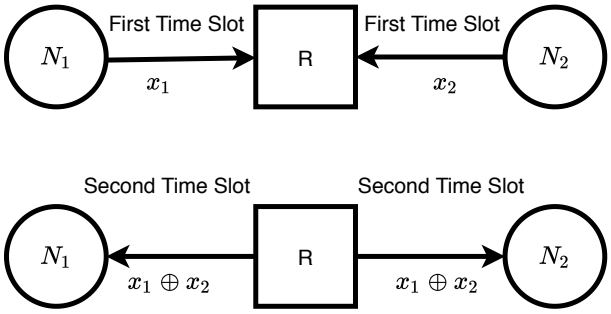

Figure 2.4. Data transmission with PNC

2.2. Physical Layer Network Coding

In the design of most of the networks, interference is treated as an unwanted situation. On the other hand, for PNC, interference is not considered as an unwanted situation. The network exploits from the interference rather than to eliminate it.

Hence, a network aware physical layer concept is defined to implement PNC in (Sykora and Burr, 2018). A network aware receiver knows its location in the network and also knows how to process the composite signal which comes from different radio links. It is capable to extract the necessary information from the sum of all information. A network aware transmitter also knows the influence of transmitting signal on the receiver. Thus, it alters its transmission parameters so that the receiver can reach the exact information correctly. A network aware physical layer allows us an efficient resource use.

Thereby, two important information theoretical terms have been given for PNC in (Sykora and Burr, 2018) such as hierarchical information (HI) and hierarchical side information (HSI). HI is the information forwarded in BC. Then, HSI is the terminal nodes' own data. HSI is used to extract other node's data from HI. For example, given in Figure 2.5 (Sykora and Burr, 2018), the terminal nodes extract the other node's data by the XOR operation of HI with their own data (HSI).

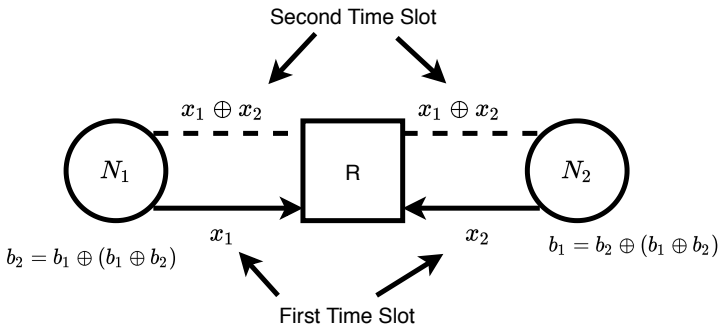

Figure 2.5. PNC in Two-way relay channel

For the rest of this section, the concept of PNC is represented for BPSK modulation. Denote b_i as the bit stream of ith terminal node $\forall i \in \{1, 2\}$ which is mapped to the transmit symbol x_i as given below:

$$x_i = \mathcal{M}_B(b_i) = 2b_i - 1 \tag{2.1}$$

In the MAC phase, the terminal nodes send their modulated signals simultaneously. After, the received signal at the relay in MAC phase is given as follows:

$$y_R = h_1 x_1 + h_2 x_2 + n \tag{2.2}$$

where n is additive white Gaussian noise (AWGN) with zero mean and power spectral density (PSD) of $\frac{N_0}{2}$. $h_i, \forall i \in \{1, 2\}$ is the ith channel gain between ith terminal node and the relay. Firstly, it is assumed to $h_1 = h_2 = 1$. According to the received constellation point, $x_1 + x_2$, the relay decides on the BPSK modulated NCS x_R. The received noiseless constellation at the relay is illustrated in Figure 2.6 (Fang, 2014).

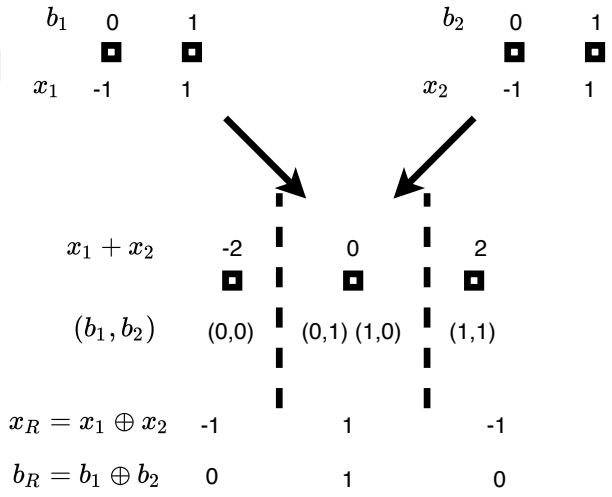

Figure 2.6. Constellation of composite signal at the relay

The relay divides the constellation into two decision regions. For the left and right regions, it decides that the NCS is -1 while for the middle region it decides that NCS is 1. As an example, when (1,0) is sent, $x_1 + x_2 = 0$ is observed at the relay. Next, this signal is directly mapped to $x_R = 1$ and broadcasted to the terminal nodes. At first node, after the detection, the data of second node can be obtained as $b_2 = 0$.

For the rest of this section, PNC with QPSK modulation is examined. The channel gains between first and second terminal nodes and the relay are assumed as 1. For this case, assume that each terminal node applies QPSK with gray encoding. Then, a new form of NCS is constructed. For this case, NCS becomes a bit pair since QPSK symbol consists of two bits. In Figure 2.7 (Fang, 2014), the constellations at terminal nodes and the received constellation at the relay with QPSK are illustrated.

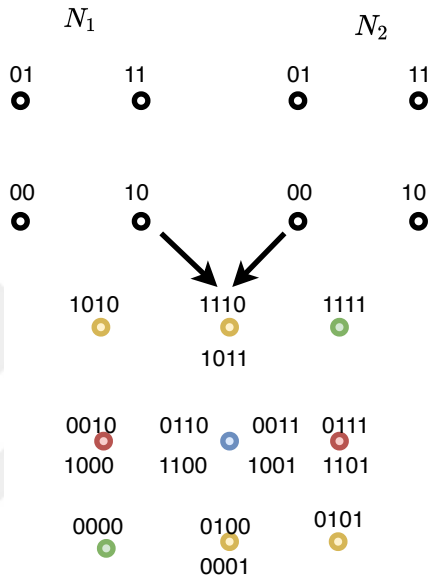

Figure 2.7. Constellation of composite signal at relay with QPSK

Hence, the constellation points which have the same color are named as clashes which are colored according to their NCSs. The colors blue, red, yellow and green stand for possible NCSs 11,10,01 and 00 respectively. For this case, since constellation points which are in same clash give identical NCS, bit-wise XOR operation can be used again as network coding operation. To give an example, consider the blue clash, for 0110, first node sends 01 and second node sends 10. After, the NCS is obtained as 11. In this clash, there are three more constellation points and three of them give the same NCS with bit-wise XOR. Let consider the case when first node sends 01 and second node sends 10. For this case, the composite symbol is 0110 which is in the blue clash and gives 11 as NCS. At node N_1, N_2's data 10 can be found by applying bit-wise XOR operation again.

2.2.1. PNC in Rayleigh Fading Channel

For the previous scenario, the channel gains between the relay and each terminal node are considered as 1. However, as a result of nature of the channel, fading is unavoidable. Let assume that the relay knows the channel coefficients h_1 and h_2 which are complex Gaussian random variables with zero mean and unity variance. The relay should decide on the NCS correctly even in the existence of fading. Decision based detection may give error because of the fading. In (Chu et al., 2017), maximum likelihood (ML) detection is applied to estimate NCS by first estimating the transmitted pairs separately. The received signal at the relay is

$$y_R = h_1 x_1 + h_2 x_2 + n \tag{2.3}$$

where y_R is the received signal, n is the AWGN at the relay, $x_i, \forall i \in \{1, 2\}$ is the transmit symbol by the ith terminal node and $h_i, \forall i \in \{1, 2\}$ is modeled by $\mathcal{CN}(0, 1)$. After, the estimated pair of transmitted symbols is obtained by

$$(\tilde{x_1}, \tilde{x_2}) = \underset{(x_1, x_2) \in \Omega}{\operatorname{argmin}} |y_R - h_1 x_1 - h_2 x_2| \tag{2.4}$$

where $\Omega = \{(-1, -1), (-1, 1), (1, -1), (1, 1)\}$ is the set of all possible pairs of x_1 and x_2 for BPSK. Then, the estimated transmit symbol is mapped to its corresponding data sequence $\tilde{b}_i, \forall i \in \{1, 2\}$ by the following map:

$$\tilde{b}_i = \begin{cases} 0, & \tilde{x}_i = -1 \\ 1, & \tilde{x}_i = 1 \end{cases} \tag{2.5}$$

Finally, the estimated NCS sequence can be obtained as follows:

$$\tilde{b}_R = \tilde{b}_1 \oplus \tilde{b}_2 \tag{2.6}$$

However, as the modulation size increases, estimation of the NCS becomes more complex because the cardinality of the set of all the possible signal pairs increases dramatically. Thus, an alternative technique has been examined for QPSK by (Sykora and Burr, 2018). First, the concept of singular fading must be explained. Singular fading occurs when some different symbol combinations result in the same constellation point. It is expressed mathematically as (Sykora and Burr, 2018):

$$\exists(x_1, x_2) \neq (x_1', x_2') : u_{1,2} = h_1 x_1 + h_2 x_2 = u_{1,2}' = h_1 x_1' + h_2 x_2' \tag{2.7}$$

In order to apply PNC, singular fading is needed to form clashes which means that the constellation must be divided into the decision regions. A suitable network coding operation for each region enables terminal nodes unambiguously decode the other terminal node's data. Let denote $h = \frac{h_2}{h_1}$ as the relative fading coefficient. When there is no fading, bit-wise XOR operation can be used as the network coding operation since each symbol combination in each clash gives the same NCS. However, as given in Figure 2.8 (Sykora and Burr, 2018), when $h \approx j$, the symbol combinations which locate at zero do not give the same NCS with bit-wise XOR. In other words, for 0010, the corresponding NCS is 10, while for 1011, it is 01.

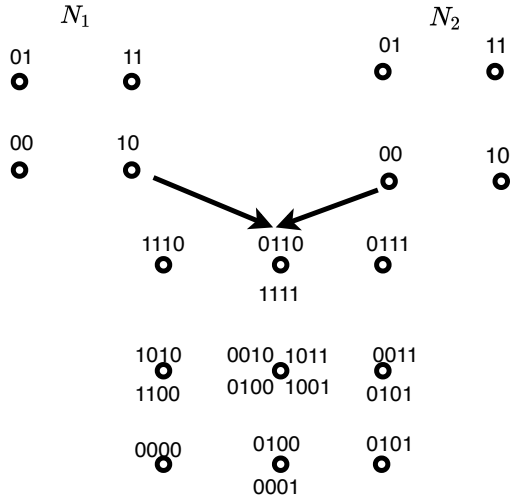

Figure 2.8. Constellation of composite signal at relay with QPSK when $h \approx j$

Instead of bit-wise XOR, a multiplication operation with a matrix, that gives same NCS for each clash, is defined for the received constellation illustrated in Figure 2.8. Hence, the corresponding matrix is represented as follows (Sykora and Burr, 2018):

$$\mathbf{G} = \begin{bmatrix} 1 & 0 & 0 & 1 \\ 0 & 1 & 1 & 0 \end{bmatrix} \tag{2.8}$$

When first node sends 00 and the second node sends 10, the combined symbol is 0010 which gives 01 as NCS given in the equation below:

$$\mathbf{s}_R = \begin{bmatrix} 1 & 0 & 0 & 1 \\ 0 & 1 & 1 & 0 \end{bmatrix} \times \begin{bmatrix} 0 \\ 0 \\ 1 \\ 0 \end{bmatrix} = \begin{bmatrix} 0 \\ 1 \end{bmatrix} \tag{2.9}$$

After, the relay sends 01 to both first terminal node and the second terminal node. For example, at first terminal node, $\mathbf{s}_1$ is merged with NCS as follows:

$$\mathbf{m} = \begin{bmatrix} 0 \\ 0 \\ 0 \\ 1 \end{bmatrix} = \begin{bmatrix} \mathbf{s}_1 \\ \mathbf{s}_R \end{bmatrix} \tag{2.10}$$

Finally, when this merged vector $\mathbf{m}$ is multiplied with $\mathbf{G}$ matrix, $\mathbf{s}_2$ can be obtained as follows:

$$\mathbf{s}_2 = \begin{bmatrix} 1 & 0 & 0 & 1 \\ 0 & 1 & 1 & 0 \end{bmatrix} \times \begin{bmatrix} 0 \\ 0 \\ 0 \\ 1 \end{bmatrix} = \begin{bmatrix} 1 \\ 0 \end{bmatrix} \tag{2.11}$$

2.2.2. BER Analysis

In this section, BER analysis of the BPSK modulation, NC and PNC in AWGN channel is examined. For BC phase, the BER is the same for all schemes and given by:

$$\mathrm{BER}_{\mathrm{BPSK}} = \mathrm{BER}_{\mathrm{NC}}^{\mathrm{BC}} = \mathrm{BER}_{\mathrm{PNC}}^{\mathrm{BC}} = Q\left(\sqrt{\frac{2E_b}{N_0}}\right). \tag{2.12}$$

Where E_b is energy per bit. For MAC phase, PNC and NC have different BER performances. For NC, the BER for the first and the second time slots are same as given in Eq.(2.12). Note that, relay performs XOR of the terminal node's data with an error if and only if one of the terminal node's data is detected with an error. If both of them are detected with an error XOR of them gives the same result as the error free case. Thus, BER of NC for MAC phase is given below (Zhang et al., 2006):

$$\mathrm{BER}_{\mathrm{NC}}^{\mathrm{MAC}} = 2Q\left(\sqrt{\frac{2E_b}{N_0}}\right)\left(1 - Q\left(\sqrt{\frac{2E_b}{N_0}}\right)\right) \tag{2.13}$$

In order to derive the BER analysis of the PNC, we first need to determine the occurrence probabilities of the constellation points at the relay when two terminal nodes use BPSK modulation. From Table 2.1, it can be observed that the occurrence probability of 0 is 0.5 while -2 and 2 have the same occurrence probabilities which are equal to 0.25.

Table 2.1. Occurrence probabilities of the received signals at the relay for BPSK

$\mathrm{p}_{x_1} = \mathrm{p}_{b_1}$	b_1	x_1	$\mathrm{p}_{x_2} = \mathrm{p}_{b_2}$	b_2	x_2	$\mathrm{p}_{x_1+x_2}$	$x_1 + x_2$	x_R	b_R
0.5	0	-1	0.5	0	-1	0.25	-2	-1	0
0.5	0	-1	0.5	1	1	0.25	0	1	1
0.5	1	1	0.5	0	-1	0.25	0	1	1
0.5	1	1	0.5	1	1	0.25	2	-1	0

According to the Table 2.1, the threshold values in the decision region $\lambda_{th,1}$ and $\lambda_{th,2}$ are determined based on the maximum posterior criterion which are defined as follows (Zhang et al., 2006):

$$\lambda_{th,1} = -1 - \frac{N_0}{4}\ln\left(1 + \sqrt{1 - \exp\left(\frac{-8}{N_0}\right)}\right) \tag{2.14}$$

and

$$\lambda_{th,2} = 1 + \frac{N_0}{4}\ln\left(1 + \sqrt{1 - \exp\left(\frac{-8}{N_0}\right)}\right) \tag{2.15}$$

Then, NCS is decided according to these threshold values. When received signal is between $\lambda_{th,1}$ and $\lambda_{th,2}$, the relay decides that NCS is 1, otherwise it equals to -1. Finally, the BER of PNC for MAC phase can be calculated as follows:

$$\begin{aligned}
\mathrm{BER}_{\mathrm{PNC}}^{\mathrm{MAC}} &= \frac{1}{2}\left(\int_{-\infty}^{\lambda_{th,1}} \frac{1}{\sqrt{\pi N_0}}\exp\left(\frac{-r^2}{N_0}\right)dr + \int_{\lambda_{th,2}}^{\infty} \frac{1}{\sqrt{\pi N_0}}\exp\left(\frac{-r^2}{N_0}\right)dr\right) \\
&\quad + \frac{1}{4}\left(\int_{\lambda_{th,1}}^{\lambda_{th,2}} \frac{1}{\sqrt{\pi N_0}}\left(\exp\left(\frac{-(r-2)^2}{N_0}\right) + \exp\left(\frac{-(r+2)^2}{N_0}\right)\right)dr\right. \\
&= \frac{1}{2}\left(Q\left(\frac{-\lambda_{th,1}}{\sqrt{N_0/2}}\right) + Q\left(\frac{\lambda_{th,2}}{\sqrt{N_0/2}}\right)\right) + \frac{1}{4}\left(Q\left(\frac{(\lambda_{th,1}-2)}{\sqrt{N_0/2}}\right) - Q\left(\frac{(\lambda_{th,2}-2)}{\sqrt{N_0/2}}\right)\right) \\
&\quad + \frac{1}{4}\left(Q\left(\frac{(\lambda_{th,1}+2)}{\sqrt{N_0/2}}\right) - Q\left(\frac{(\lambda_{th,2}+2)}{\sqrt{N_0/2}}\right)\right)
\end{aligned} \tag{2.16}$$

2.3. PNC for Multi-user Massive MIMO systems

In this section, PNC for multi-user massive MIMO systems are examined. Since the critical point for both PNC and NC is to estimate the NCS, we focus on MAC phase. First, the system model is given. Then, the estimation of NCS for NC and PNC with linear detection is examined. Next, MAC phases of PNC and NC are presented with

the users having different SNR values. After, we propose a technique to estimate NCS without using LLR which decreases the complexity. Finally, the performance evaluations are given.

Up to this section, all nodes are named as relay and terminal node. From this point, we denote the relay as BS and terminal nodes as UEs.

2.3.1. System Model

The system model given in Figure 2.9 consists of one BS and K UEs. Through PNC, each UE extracts the other UE's modulated data pairwise with the help of BS. Thus, they form $K_p = \frac{K}{2}$ user pairs. The BS is equipped with M antennas while each UE has N antennas and $L = KN$ is the total number of transmit antennas by all UEs. For this section, our system is modeled such that $M = L$.

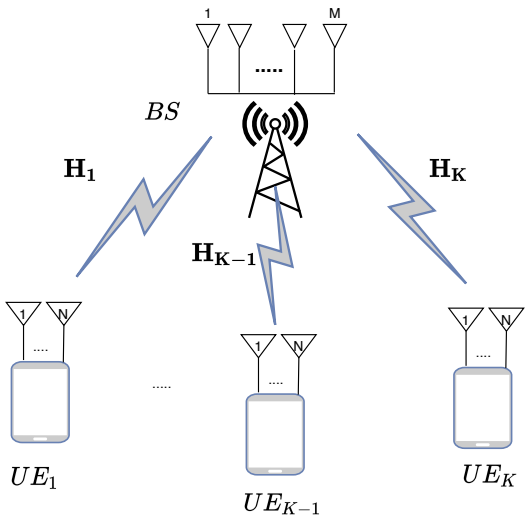

Figure 2.9. System Model for multi-user massive MIMO-PNC

The received vector at BS is given as follows:

$$\mathbf{r} = \mathbf{H}\sqrt{\mathbf{\Gamma}}\mathbf{x} + \mathbf{n} \tag{2.17}$$

where $\mathbf{\Gamma} = \text{diag}(\Gamma_1 \mathbf{I}_N, \cdots, \Gamma_K \mathbf{I}_N)$ includes the path loss coefficients effecting the symbols of kth user $\forall k \in \{1, 2, \cdots, K\}$, note that each symbol transmitted from kth user experiences the same pathloss coefficient which is Γ_k, $\mathbf{H}$ is the composite channel matrix, $\mathbf{n}$ is the noise vector, $\mathbf{x}$ is the composite transmit symbol vector.

The composite channel matrix $\mathbf{H}$ is formed by considering all channel matrices between UEs and BS described by:

$$\mathbf{H} = \begin{bmatrix} \mathbf{H}_1 & \mathbf{H}_2 & \cdots & \mathbf{H}_K \end{bmatrix}_{M \times L} \tag{2.18}$$

where $\mathbf{H}_k \in \mathbb{C}^{M \times N}$ is the channel matrix between kth user UE_k and the BS whose entries are the complex Gaussian random variables which have zero mean and unity variance. Then, the channel composite matrix is constrained as follows:

$$\mathbb{E}\{||\mathbf{H}||_F^2\} = \text{tr}\{\mathbb{E}\{\mathbf{H}\mathbf{H}^H\}\} = ML \tag{2.19}$$

The composite transmit symbol vector $\mathbf{x}$ is given below:

$$\mathbf{x} = \begin{bmatrix} \mathbf{x}_1 & \mathbf{x}_2 & \cdots & \mathbf{x}_K \end{bmatrix}^T \tag{2.20}$$

where $\mathbf{x}_k = \begin{bmatrix} x_{k_1} & x_{k_2} & \cdots & x_{k_N} \end{bmatrix}$ is the transmit symbol vector from UE_k where each x_{k_i} is the transmit symbol from the ith antenna of the kth user $\forall k \in \{1, 2, \cdots, K\}$ and $\forall i \in \{1, 2, \cdots, N\}$.

Then, the power of the composite transmit symbol vector is constrained as:

$$\mathbb{E}\{||\mathbf{x}||^2\} \leq \text{P} \tag{2.21}$$

where P is the total transmit power by all users.

The average received power for kth user is given by,

$$\mathbb{E}\{|\sqrt{\Gamma_k}\mathbf{x}_k|^2\}) = \text{p}_\text{k} \tag{2.22}$$

After, the auto covariance matrix of the composite transmit symbol vector $\mathbf{x}$ is given as follows:

$$\mathbb{E}\{\mathbf{x}\mathbf{x}^H\} = \frac{\mathrm{P}}{L}\mathbf{I}_{L\times L} \tag{2.23}$$

Finally, $\mathbf{n}$ is the AWGN vector and modeled by $\mathbf{n} \sim \mathcal{CN}(\mathbf{0}_M, \sigma_n^2\mathbf{I}_M)$, which is expressed as below:

$$\mathbf{n} = \begin{bmatrix} n_1 & n_2 & \cdots & n_M \end{bmatrix}^T \tag{2.24}$$

Then, the averaged received SNR belonging to the kth user is defined by,

$$\gamma_k = \frac{M\mathrm{p_k}}{\sigma_n^2} \tag{2.25}$$

When the transmit power is equally shared between the users and their path loss gains are set to unity for the sake of simplicity, the averaged received SNR at the BS per antenna is written as follows:

$$\gamma_0 = \frac{M}{L}\frac{\mathrm{P}}{\sigma_n^2} \tag{2.26}$$

For this section, the following assumptions are hold. The BS has the perfect channel state information (CSI) about the channel between all UEs and itself. There is a perfect synchronization between each user and the BS and all UEs send their data to the BS simultaneously. All users modulate their data with a reverse mapping of BPSK.

2.3.2. MIMO-NC scheme based on Linear Detection

For this section, the estimation of NCS vector with dimension $Q = \frac{L}{2}$ in MIMO-NC is examined. The corresponding NCS vector is defined as follows:

$$\mathbf{x}_R = \begin{bmatrix} x_1 \oplus x_{Q+1} \\ x_2 \oplus x_{Q+2} \\ \cdots \\ x_Q \oplus x_{2Q} \end{bmatrix} = \begin{bmatrix} x_{R_1} \\ x_{R_2} \\ \cdots \\ x_{R_Q} \end{bmatrix} \tag{2.27}$$

Firstly, the received vector $\mathbf{r}$ is equalized by using linear detection techniques as follows:

$$\mathbf{y} = \mathbf{G}\mathbf{r} \tag{2.28}$$

Then, Eq.(2.28) is given explicitly by:

$$\mathbf{y} = \mathbf{G}\mathbf{H}\mathbf{x} + \mathbf{G}\mathbf{n} \tag{2.29}$$

where $\mathbf{G}$ and $\mathbf{y}$ are the equalization matrix and the equalized vector respectively.

For the ZF solution, $\mathbf{G}$ is the pseudo inverse of the composite channel matrix $\mathbf{H}$ which is given by the following equation (Van Loan and Golub, 1983):

$$\mathbf{G} = (\mathbf{H})^{\dagger} = (\mathbf{H}^H\mathbf{H})^{-1}\mathbf{H}^H \tag{2.30}$$

Theorem 2.3.1 *The equalization matrix for NC with MMSE* $\mathbf{G}$*, is expressed below (Kay, 1993):*

$$\mathbf{G} = (\mathbf{H}^H\mathbf{H} + \frac{1}{\gamma_0}\mathbf{I}_{L\times L})^{-1}\mathbf{H}^H \tag{2.31}$$

Proof

In order to estimate $\mathbf{x}$, a matrix $\mathbf{G}$ is needed which satisfies $\mathbf{G}\mathbf{r} = \mathbf{x}$. Error vector is defined as $\mathbf{e} = \mathbf{G}\mathbf{r} - \mathbf{x}$. Since the correlation between the error and the received vector must be zero for the MMSE solution, equalization matrix $\mathbf{G}$ is given by solving the equation below:

$$\mathbb{E}\{\mathbf{e}\mathbf{r}^H\} = 0 \tag{2.32}$$

Hence, Eq.(2.32) can be arranged as:

$$\mathbf{G} = \mathbb{E}\{\mathbf{x}\mathbf{r}^H\}\mathbb{E}\{\mathbf{r}\mathbf{r}^H\}^{-1} \tag{2.33}$$

After, the auto covariance matrix of the received vector $\mathbb{E}\{\mathbf{r}\mathbf{r}^H\}$ in Eq.(2.33) can be expressed explicitly as follows:

$$\mathbb{E}\{\mathbf{r}\mathbf{r}^H\} = \mathbb{E}\{(\mathbf{H}\mathbf{x} + \mathbf{n})(\mathbf{H}\mathbf{x} + \mathbf{n})^H\} \tag{2.34}$$

Following the algebraic manipulations, the expression in Eq.(2.34) can be revised as follows:

$$\mathbb{E}\{\mathbf{r}\mathbf{r}^H\} = \mathbb{E}\{\mathbf{H}\mathbf{x}\mathbf{x}^H\mathbf{H}^H\} + \mathbb{E}\{\mathbf{n}\mathbf{x}^H\mathbf{H}^H\} + \mathbb{E}\{\mathbf{H}\mathbf{x}\mathbf{n}^H\} + \mathbb{E}\{\mathbf{n}\mathbf{n}^H\} \tag{2.35}$$

Knowing that the correlation between $\mathbf{n}$ and $\mathbf{x}$ is zero, $\mathbb{E}\{\mathbf{r}\mathbf{r}^H\}$ in Eq.(2.35) becomes:

$$\mathbb{E}\{\mathbf{r}\mathbf{r}^H\} = \mathbb{E}\{\mathbf{H}\mathbf{x}\mathbf{x}^H\mathbf{H}^H\} + \mathbb{E}\{\mathbf{n}\mathbf{n}^H\} \tag{2.36}$$

Knowing that the auto covariance matrix of the noise vector is $\sigma_n^2\mathbf{I}_{M\times M}$ and by using the constraint on $\mathbf{H}$ in Eq.(2.19), the auto covariance matrix of the received vector in Eq.(2.36) is given as:

$$\mathbb{E}\{\mathbf{r}\mathbf{r}^H\} = M\mathbf{H}\mathbb{E}\{\mathbf{x}\mathbf{x}^H\}\mathbf{H}^H + \sigma_n^2\mathbf{I}_{M\times M} \tag{2.37}$$

Owing to $\mathbb{E}\{\mathbf{x}\mathbf{x}^H\} = \dfrac{\mathrm{P}}{L}\mathbf{I}_{L\times L}$, by Eq.(2.23), the auto covariance matrix of the received vector in Eq.(2.37) becomes:

$$\mathbb{E}\{\mathbf{r}\mathbf{r}^H\} = \frac{\mathrm{P}}{L}\mathbf{H}\mathbf{H}^H + \sigma_n^2\mathbf{I}_{M\times M} \tag{2.38}$$

Thereby, the explicit expression for $\mathbb{E}\{\mathbf{x}\mathbf{r}^H\}$, can be obtained as:

$$\mathbb{E}\{\mathbf{x}\mathbf{r}^H\} = \mathbb{E}\{\mathbf{x}(\mathbf{H}\mathbf{x} + \mathbf{n})^H\} \tag{2.39}$$

After the multiplication operation is performed in Eq.(2.39), the correlation between the transmit vector and the received vector is rewritten as:

$$\mathbb{E}\{\mathbf{x}\mathbf{r}^H\} = \mathbb{E}\{\mathbf{x}\mathbf{x}^H\mathbf{H}^H\} + \mathbb{E}\{\mathbf{x}\mathbf{n}^H\} \tag{2.40}$$

Knowing the correlation between $\mathbf{n}$ and $\mathbf{x}$ is zero in Eq.(2.40), the expression for $\mathbb{E}\{\mathbf{x}\mathbf{r}^H\}$ becomes:

$$\mathbb{E}\{\mathbf{x}\mathbf{r}^H\} = \mathbb{E}\{\mathbf{x}\mathbf{x}^H\}\mathbf{H}^H = M\frac{\mathrm{P}}{L}\mathbf{H}^H \tag{2.41}$$

If Eq.(2.38) and Eq.(2.41) are combined and using the SNR value in Eq.(2.26), the final expression for the equalization matrix is described by:

$$\mathbf{G} = (\mathbf{H}^H\mathbf{H} + \frac{1}{\gamma_0}\mathbf{I}_{L\times L})^{-1}\mathbf{H}^H \tag{2.42}$$

End of the Proof

After that, each transmit symbol for each UE is estimated from the estimated symbol $\mathbf{y}$ according to the following rule:

$$\tilde{x}_l = \begin{cases} -1, & y_l > 0 \\ 1, & y_l \leq 0 \end{cases}, \quad \forall l \in \{1, 2, \cdots, 2Q\} \tag{2.43}$$

Finally, qth element of NCS vector in Eq.(2.27), is obtained by

$$x_{R_q} = \tilde{x}_q \oplus \tilde{x}_{q+Q}, \quad \forall q \in \{1, 2, \cdots, Q\} \tag{2.44}$$

where $\oplus$ operation is the baseband equivalent XOR operation which is actually multiplication of two symbols.

2.3.3. MIMO-PNC scheme based on Linear Detection

For this section, the estimation of the NCS vector for PNC is examined. Firstly, the received vector in Eq.(2.17) can be rewritten as follows (Zhang and Liew, 2010):

$$\mathbf{r} = \mathbf{H}\mathbf{D}^{-1}\mathbf{D}\mathbf{x} + \mathbf{n} \tag{2.45}$$

Then, Eq.(2.45) is rewritten by the following equation:

$$\mathbf{r} = \hat{\mathbf{H}}\hat{\mathbf{x}} + \mathbf{n} \tag{2.46}$$

where the reformed composite channel matrix $\hat{\mathbf{H}}$ is represented as:

$$\hat{\mathbf{H}} = \mathbf{H}\mathbf{D}^{-1} \tag{2.47}$$

Then, the estimated symbol vector $\hat{\mathbf{x}}$, whose elements are the sums and the differences of the user pairs' transmitted symbols, is defined followed by:

$$\hat{\mathbf{x}} = \mathbf{D}\mathbf{x} \tag{2.48}$$

$\mathbf{D}$ is the sum difference matrix which can be expressed by:

$$\mathbf{D} = \begin{bmatrix} \mathbf{I}_{Q\times Q} & \mathbf{I}_{Q\times Q} \\ \mathbf{I}_{Q\times Q} & -\mathbf{I}_{Q\times Q} \end{bmatrix} \tag{2.49}$$

$\hat{\mathbf{x}}$ can be expressed in the vector form followed by:

$$\hat{\mathbf{x}} = \begin{bmatrix} x_1 + x_{Q+1} \\ x_2 + x_{Q+2} \\ \cdots \\ x_Q + x_{2Q} \\ x_1 - x_{Q+1} \\ x_2 - x_{Q+2} \\ \cdots \\ x_Q - x_{2Q} \end{bmatrix} \tag{2.50}$$

After, the equalized vector is obtained by:

$$\mathbf{y} = \hat{\mathbf{G}}\mathbf{r} \tag{2.51}$$

Then, Eq.(2.51) is given explicitly by:

$$\mathbf{y} = \hat{\mathbf{G}}\hat{\mathbf{H}}\hat{\mathbf{x}} + \mathbf{n} \tag{2.52}$$

where $\hat{\mathbf{G}}$ and $\hat{\mathbf{y}}$ are the equalization matrix and equalized vector respectively for PNC.

Theorem 2.3.2 *The equalization matrix for PNC with ZF* $\hat{\mathbf{G}}$*, is pseudo inverse of the reformed composite channel matrix* $\hat{\mathbf{H}}$ *which is given as follows:*

$$\hat{\mathbf{G}} = (\hat{\mathbf{H}})^{\dagger} = (\hat{\mathbf{H}}^{H}\hat{\mathbf{H}})^{-1}\hat{\mathbf{H}}^{H} \tag{2.53}$$

Proof

For the ZF solution, the norm of the error vector is defined as: $||\mathbf{e}|| = ||\mathbf{r} - \hat{\mathbf{H}}\hat{\mathbf{x}}||$. Then, in order to find the expression that minimizes the square of the norm of the error vector $||\mathbf{e}||^2 = ||\mathbf{r} - \hat{\mathbf{H}}\hat{\mathbf{x}}||^2$, the derivative of this expression must be taken and equated to the zero as:

$$\frac{d}{d\hat{\mathbf{x}}}(||\mathbf{r} - \hat{\mathbf{H}}\hat{\mathbf{x}}||^2) = 0 \tag{2.54}$$

Next, the norm squared term in Eq.(2.54) can be expanded as follows:

$$\frac{d}{d\hat{\mathbf{x}}}((\mathbf{r} - \hat{\mathbf{H}}\hat{\mathbf{x}})^{H}(\mathbf{r} - \hat{\mathbf{H}}\hat{\mathbf{x}})) = 0 \tag{2.55}$$

After the expansion of the multiplication, Eq.(2.55) is given by:

$$\frac{d}{d\hat{\mathbf{x}}}(\mathbf{r}^{H}\mathbf{r} - \hat{\mathbf{x}}^{H}\hat{\mathbf{H}}\mathbf{r} - \mathbf{r}^{H}\hat{\mathbf{H}}\hat{\mathbf{x}} + \hat{\mathbf{x}}^{H}\hat{\mathbf{H}}^{H}\hat{\mathbf{H}}\hat{\mathbf{x}}) = 0 \tag{2.56}$$

After the arrangement of Eq.(2.56), we obtain $-2\hat{\mathbf{H}}^{H}\mathbf{r} + 2\hat{\mathbf{H}}^{H}\hat{\mathbf{H}}\hat{\mathbf{x}} = 0$. Hence, the final expression for $\tilde{\hat{\mathbf{x}}}$ becomes $\tilde{\hat{\mathbf{x}}} = \underbrace{(\hat{\mathbf{H}}^{H}\hat{\mathbf{H}})^{-1}\hat{\mathbf{H}}}_{\hat{\mathbf{G}}}\mathbf{r}$. Finally, the equalization matrix for the ZF is represented by the following equation:

$$\hat{\mathbf{G}} = (\hat{\mathbf{H}}^{H}\hat{\mathbf{H}})^{-1}\hat{\mathbf{H}}^{H} \tag{2.57}$$

End of the Proof

Theorem 2.3.3 *The equalization matrix for PNC with MMSE* $\hat{\mathbf{G}}$*, is obtained by the following equation:*

$$\hat{\mathbf{G}} = (\hat{\mathbf{H}}^H\hat{\mathbf{H}} + \frac{1}{2\gamma_0}\mathbf{I}_{L\times L})^{-1}\hat{\mathbf{H}}^H \tag{2.58}$$

Proof

$\hat{\mathbf{x}}$ is subject to be estimated, so a matrix $\hat{\mathbf{G}}$ which satisfies $\hat{\mathbf{G}}\mathbf{r} = \hat{\mathbf{x}}$ is required. Define the error vector as $\mathbf{e} = \hat{\mathbf{G}}\mathbf{r} - \hat{\mathbf{x}}$. Since the correlation between the error and the received vector must be zero for MMSE solution, $\hat{\mathbf{G}}$ can be obtained by solving the following equation:

$$\mathbb{E}\{\mathbf{e}\mathbf{r}^H\} = 0 \tag{2.59}$$

Next, by arranging Eq.(2.59), the equalization matrix $\hat{\mathbf{G}}$ can be obtained as

$$\hat{\mathbf{G}} = \mathbb{E}\{\hat{\mathbf{x}}\mathbf{r}^H\}\mathbb{E}\{\mathbf{r}\mathbf{r}^H\}^{-1} \tag{2.60}$$

First, the term $\mathbb{E}\{\mathbf{r}\mathbf{r}^H\}$ in Eq.(2.60) can be expressed explicitly by the following equation

$$\mathbb{E}\{\mathbf{r}\mathbf{r}^{\mathbf{H}}\} = \mathbb{E}\{(\hat{\mathbf{H}}\hat{\mathbf{x}} + \mathbf{n})(\hat{\mathbf{H}}\hat{\mathbf{x}} + \mathbf{n})^H\} \tag{2.61}$$

After the expansion of the multiplication in Eq.(2.61), the expression for the auto covariance matrix of the received vector is:

$$\mathbb{E}\{\mathbf{r}\mathbf{r}^H\} = \mathbb{E}\{\hat{\mathbf{H}}\hat{\mathbf{x}}\hat{\mathbf{x}}^H\hat{\mathbf{H}}^H\} + \mathbb{E}\{\mathbf{n}\hat{\mathbf{x}}^H\hat{\mathbf{H}}^H\} + \mathbb{E}\{\hat{\mathbf{H}}\hat{\mathbf{x}}\mathbf{n}^H\} + \mathbb{E}\{\mathbf{n}\mathbf{n}^H\} \tag{2.62}$$

Due to the zero correlation between $\mathbf{n}$ and $\hat{\mathbf{x}}$, Eq.(2.62) becomes:

$$\mathbb{E}\{\mathbf{r}\mathbf{r}^H\} = \mathbb{E}\{\hat{\mathbf{H}}\hat{\mathbf{x}}\hat{\mathbf{x}}^H\hat{\mathbf{H}}^H\} + \mathbb{E}\{\mathbf{n}\mathbf{n}^H\} \tag{2.63}$$

Knowing that the auto covariance matrix of the noise vector is $\sigma_n^2\mathbf{I}_{M\times M}$ and by using the constraint on $\mathbf{H}$ in Eq.(2.19), the expression for $\mathbb{E}\{\mathbf{r}\mathbf{r}^H\}$ is given as:

$$\mathbb{E}\{\mathbf{r}\mathbf{r}^H\} = M\hat{\mathbf{H}}\mathbb{E}\{\hat{\mathbf{x}}\hat{\mathbf{x}}^H\}\hat{\mathbf{H}}^H + \sigma_n^2\mathbf{I}_{M\times M}. \tag{2.64}$$

Hence, the final expression for the auto covariance matrix of the estimated vector $\mathbb{E}\{\hat{\mathbf{x}}\hat{\mathbf{x}}^H\}$, can be described by following the equation $\mathbb{E}\{\hat{\mathbf{x}}\hat{\mathbf{x}}^H\} = \mathbb{E}\{(\mathbf{D}\mathbf{x})(\mathbf{D}\mathbf{x})^H\}$. Since, $\mathbf{D}$ is a deterministic matrix, it can be taken out from the expectation operator as follows $\mathbb{E}\{\hat{\mathbf{x}}\hat{\mathbf{x}}^H\} = \mathbf{D}\mathbb{E}\{\mathbf{x}\mathbf{x}^H\}\mathbf{D}^H$. Knowing $\mathbb{E}\{\mathbf{x}\mathbf{x}^H\} = \frac{\mathrm{P}}{L}\mathbf{I}_{L\times L}$ by Eq.(2.23), the auto covariance of $\hat{\mathbf{x}}$ can be rewritten as $\mathbb{E}\{\hat{\mathbf{x}}\hat{\mathbf{x}}^H\} = \frac{\mathrm{P}}{L}\mathbf{D}\mathbf{I}\mathbf{D}^H$. Since $\mathbf{D}\mathbf{D}^H = 2\mathbf{I}_{L\times L}$, the auto covariance of $\hat{\mathbf{x}}$ is $\mathbb{E}\{\hat{\mathbf{x}}\hat{\mathbf{x}}^H\} = \frac{2\mathrm{P}}{L}\mathbf{I}_{L\times L}$ Then, the auto covariance matrix of the received vector is expressed as:

$$\mathbb{E}\{\mathbf{r}\mathbf{r}^H\} = \frac{2M\mathrm{P}}{L}\hat{\mathbf{H}}\hat{\mathbf{H}}^H + \sigma_n^2\mathbf{I}_{M\times M} \tag{2.65}$$

After, the explicit expression for $\mathbb{E}\{\hat{\mathbf{x}}\mathbf{r}^H\}$ can be obtained by the following equation:

$$\mathbb{E}\{\hat{\mathbf{x}}\mathbf{r}^H\} = \mathbb{E}\{\hat{\mathbf{x}}(\hat{\mathbf{H}}\hat{\mathbf{x}} + \mathbf{n})^H\} \tag{2.66}$$

Next, Eq.(2.66) is expanded as follows:

$$\mathbb{E}\{\hat{\mathbf{x}}\mathbf{r}^H\} = \mathbb{E}\{\hat{\mathbf{x}}\hat{\mathbf{x}}^H\hat{\mathbf{H}}^H\} + \mathbb{E}\{\hat{\mathbf{x}}\mathbf{n}^H\} \tag{2.67}$$

The correlation between $\mathbf{n}$ and $\hat{\mathbf{x}}$ is zero then the expression for $\mathbb{E}\{\hat{\mathbf{x}}\mathbf{r}^H\}$ in Eq.(2.67) becomes $\mathbb{E}\{\hat{\mathbf{x}}\hat{\mathbf{x}}^H\}\hat{\mathbf{H}}^H$. Since $\mathbb{E}\{\hat{\mathbf{x}}\hat{\mathbf{x}}^H\} = \frac{2\mathrm{P}}{L}\mathbf{I}_{L\times L}$, the correlation between received vector and $\hat{\mathbf{x}}$ becomes:

$$\mathbb{E}\{\hat{\mathbf{x}}\mathbf{r}^H\} = M\frac{2\mathrm{P}}{L}\hat{\mathbf{H}}^H \tag{2.68}$$

If Eq.(2.65) and Eq.(2.68) are combined, the final expression for the equalization matrix $\hat{\mathbf{G}}$ is obtained by the following equation:

$$\hat{\mathbf{G}} = M\frac{2\mathrm{P}}{L}\hat{\mathbf{H}}^H(\frac{2M\mathrm{P}}{L}\hat{\mathbf{H}}\hat{\mathbf{H}}^H + \sigma_n^2\mathbf{I}_{M\times M})^{-1} \tag{2.69}$$

When $\frac{2M\mathrm{P}}{L}$ is taken as common factor, the expression for $\hat{\mathbf{G}}$ is

$$M\frac{2\mathrm{P}}{L}\hat{\mathbf{H}}^H(\frac{2M\mathrm{P}}{L}(\hat{\mathbf{H}}\hat{\mathbf{H}}^H + \frac{L\sigma_n^2}{2\mathrm{P}}\mathbf{I}_{M\times M}))^{-1} \tag{2.70}$$

After the term $\frac{2M\mathrm{P}}{L}$ can be taken out of the inverse operation as $\frac{\mathrm{L}}{2PM}$ and the simplifications are hold as $\hat{\mathbf{H}}^H(\hat{\mathbf{H}}\hat{\mathbf{H}}^H + \frac{L\sigma_n^2}{2\mathrm{P}M}\mathbf{I}_{M\times M})^{-1}$.

Finally, knowing the SNR value γ_0 in Eq.(2.26) we obtain the equalization matrix for PNC with MMSE $\hat{\mathbf{G}}$ as:

$$\hat{\mathbf{G}} = (\hat{\mathbf{H}}^H\hat{\mathbf{H}} + \frac{1}{2\gamma_0}\mathbf{I}_{L\times L})^{-1}\hat{\mathbf{H}}^H \tag{2.71}$$

End of the Proof

After, likelihood ratio (LR) value of the transmitted symbol pair is defined as follows (Zhang and Liew, 2010):

$$\mathrm{L}(x_q \oplus x_{q+Q}|y_q, y_{q+Q}) = \frac{\mathrm{P}(y_q, y_{q+Q}|x_q \oplus x_{q+Q} = 1)}{\mathrm{P}(y_q, y_{q+Q}|x_q \oplus x_{q+Q} = -1)}, \quad \forall q \in \{1, 2, \cdots, Q\} \tag{2.72}$$

Theorem 2.3.4 *LLR value of qth and $(q+Q)$th symbol is defined as follows:*

$$\mathrm{LLR}_q = \log\left(\mathrm{e}^{\left(\frac{2}{\sigma_q^2}-\frac{2}{\sigma_{q+Q}^2}\right)}\left(\frac{\cosh\left(\frac{2y_{q+Q}}{\sigma_{q+Q}^2}\right)}{\cosh\left(\frac{2y_q}{\sigma_q^2}\right)}\right)\right), \quad \forall q \in \{1,2,\cdots,Q\} \tag{2.73}$$

where y_q and y_{q+Q} are the elements of the equalized vector $\mathbf{y}$ given in Eq.(2.51) while σ_q^2 and σ_{q+Q}^2 are the noise variances after the equalization which can be given by:

$$\sigma_\ell^2 = \{\hat{\mathbf{G}}\hat{\mathbf{G}}^H\}_{\ell,\ell}\sigma_n^2, \quad \forall \ell \in \{1,2,\cdots L\}. \tag{2.74}$$

Proof

Since the elements of $\hat{\mathbf{x}}$ are correlated with each other, they can be transformed to NCS by $(x_q \oplus x_{q+Q})$, $\forall q \in \{1,2,\cdots,Q\}$. The information from y_q and y_{q+Q} is combined by applying LR of the NCS so that the relay estimate NCS (Zhang and Liew, 2010). Then, LR of NCS conditioning on qth and $(q+Q)$th transmit symbol is defined as follows (Zhang and Liew, 2010):

$$\mathrm{L}(x_q \oplus x_{q+Q}|y_q, y_{q+Q}) = \frac{\mathrm{P}(y_q, y_{q+Q}|x_q \oplus x_{q+Q} = 1)}{\mathrm{P}(y_q, y_{q+Q}|x_q \oplus x_{q+Q} = -1)}, \quad \forall q \in \{1,2,\cdots,Q\} \tag{2.75}$$

By the total probability principle, Eq.(2.75) can be expanded as

$$\mathrm{L} = \frac{[\mathrm{P}(y_q|\hat{x}_q = 2) + \mathrm{P}(y_q|\hat{x}_q = -2)]\mathrm{P}(y_{q+Q}|\hat{x}_{q+Q} = 0)}{\mathrm{P}(y_q|\hat{x}_q = 0)[\mathrm{P}(y_{q+Q}|\hat{x}_{q+Q} = 2) + \mathrm{P}(y_{q+Q}|\hat{x}_{q+Q} = -2)]} \tag{2.76}$$

Since, LR is formed by the conditional PDFs of y_q and y_{q+Q}, random behavior of $\mathbf{y}$ is required to figure out. When $\mathbf{r}$ is multiplied with $\hat{\mathbf{G}}$, estimate of $\hat{\mathbf{x}}$ can be found with an additive colored noise given in Eq.(2.51). Since the distribution of the noise is Gaussian, the distribution of y_q and y_{q+Q} are also Gaussian with means $\hat{x}_q$, $\hat{x}_{q+Q}$ and with variances σ_q^2, σ_{q+Q}^2 respectively. Then, PDFs of y_q and y_{q+Q} can be described as follows:

$$P(y_\ell) = \frac{1}{\sqrt{2\pi\sigma_\ell^2}}\exp\left(-\frac{(y_\ell - \hat{x_\ell})^2}{2\sigma_\ell^2}\right), \quad \forall \ell \in \{1,2,\cdots,2Q\} \tag{2.77}$$

Hence, the Eq.(2.76) can be revised as follows:

$$\mathrm{L} = \frac{\exp\Big(-\frac{y_q^2}{2\sigma_q^2}\Big)\Big(\exp\Big(-\frac{(y_{q+Q}+2)^2}{2\sigma_{q+Q}^2}\Big)+\exp\Big(-\frac{(y_{q+Q}-2)^2}{2\sigma_{q+Q}^2}\Big)\Big)}{\exp\Big(-\frac{y_{q+Q}^2}{2\sigma_{q+Q}^2}\Big)\Big(\exp\Big(-\frac{(y_q+2)^2}{2\sigma_q^2}\Big)+\exp\Big(-\frac{(y_q-2)^2}{2\sigma_q^2}\Big)\Big)} \tag{2.78}$$

If the squared terms are expanded, LR becomes:

$$\mathrm{L} = \frac{\exp\Big(-\frac{y_q^2}{2\sigma_q^2}\Big)\Big[\exp\Big(-\frac{(y_{q+Q}^2+4y_{q+Q}+4)}{2\sigma_{q+Q}^2}\Big)+\exp\Big(-\frac{(y_{q+Q}^2-4y_{q+Q}+4)}{2\sigma_{q+Q}^2}\Big)\Big]}{\exp\Big(-\frac{y_{q+Q}^2}{2\sigma_{q+Q}^2}\Big)\Big[\exp\Big(-\frac{(y_q^2+4y_q+4)}{2\sigma_q^2}\Big)+\exp\Big(-\frac{(y_q^2-4y_q+4)}{2\sigma_q^2}\Big)\Big]} \tag{2.79}$$

Next, the common terms can be taken out as follows:

$$\mathrm{L} = \frac{\exp\Big(-\frac{y_q^2}{2\sigma_q^2}\Big)\Big\{\exp\Big(\frac{-y_{q+Q}^2-4}{2\sigma_{q+Q}^2}\Big)\Big[\exp\Big(\frac{2y_{q+Q}}{\sigma_{q+Q}^2}\Big)+\exp\Big(-\frac{2y_{q+Q}}{\sigma_{q+Q}^2}\Big)\Big]\Big\}}{\exp\Big(-\frac{y_{q+Q}^2}{2\sigma_{q+Q}^2}\Big)\Big\{\exp\Big(\frac{-y_q^2-4}{2\sigma_q^2}\Big)\Big[\exp\Big(\frac{2y_q}{\sigma_q^2}\Big)+\exp\Big(-\frac{2y_q}{\sigma_q^2}\Big)\Big]\Big\}} \tag{2.80}$$

Then, a further explicit expression is obtained as:

$$\mathrm{L} = \frac{\exp\Big(-\frac{y_q^2}{2\sigma_q^2}\Big)\Big\{\exp\Big(\frac{-y_{q+Q}^2}{2\sigma_{q+Q}^2}\Big)\exp\Big(\frac{-4}{2\sigma_{q+Q}^2}\Big)\Big[\exp\Big(\frac{2y_{q+Q}}{\sigma_{q+Q}^2}\Big)+\exp\Big(-\frac{2y_{q+Q}}{\sigma_{q+Q}^2}\Big)\Big]\Big\}}{\exp\Big(-\frac{y_{q+Q}^2}{2\sigma_{q+Q}^2}\Big)\Big\{\exp\Big(\frac{-y_q^2}{2\sigma_q^2}\Big)\exp\Big(\frac{-4}{2\sigma_q^2}\Big)\Big[\exp\Big(\frac{2y_q}{\sigma_q^2}\Big)+\exp\Big(-\frac{2y_q}{\sigma_q^2}\Big)\Big]\Big\}} \tag{2.81}$$

After the simplifications of the same expressions, LR can be obtained as follows:

$$\mathrm{L} = \frac{\exp\Big(-\frac{2}{\sigma_{q+Q}^2}\Big)\Big(\exp\Big(\frac{2y_{q+Q}}{\sigma_{q+Q}^2}\Big)+\exp\Big(-\frac{2y_{q+Q}}{\sigma_{q+Q}^2}\Big)\Big)}{\exp\Big(-\frac{2}{\sigma_q^2}\Big)\Big(\exp\Big(\frac{2y_q}{\sigma_q^2}\Big)+\exp\Big(-\frac{2y_q}{\sigma_q^2}\Big)\Big)} \tag{2.82}$$

Then, LR can be rewritten as:

$$\mathrm{L} = \exp\left(\frac{2}{\sigma_q^2} - \frac{2}{\sigma_{q+Q}^2}\right)\left(\frac{\cosh\left(\frac{2y_{q+Q}}{\sigma_{q+Q}^2}\right)}{\cosh\left(\frac{2y_q}{\sigma_q^2}\right)}\right) \tag{2.83}$$

where $\cosh$ is the hyperbolic cosine function. Finally, when the logarithm of both sides is taken, the LLR can be obtained as follows:

$$\mathrm{LLR} = \log\left(\exp\left(\frac{2}{\sigma_q^2} - \frac{2}{\sigma_{q+Q}^2}\right)\left(\frac{\cosh\left(\frac{2y_{q+Q}}{\sigma_{q+Q}^2}\right)}{\cosh\left(\frac{2y_q}{\sigma_q^2}\right)}\right)\right) \tag{2.84}$$

End of the Proof

Then, (Okyere et al., 2019) made a further approximation on LLR as follows:

$$\mathrm{LLR}_q = \mathrm{LL}_q - \mathrm{LL}_{q+Q} \tag{2.85}$$

where

$$\mathrm{LL}_q \approx \max\left(\frac{2y_q - 2}{\sigma_q^2},\ \frac{-2y_q - 2}{\sigma_q^2}\right) + \log\left(1 + e^{-\left|\frac{4y_q}{\sigma_q^2}\right|}\right) \tag{2.86}$$

and

$$\mathrm{LL}_{q+Q} \approx \max\left(\frac{2y_{q+Q} - 2}{\sigma_{q+Q}^2},\ \frac{-2y_{q+Q} - 2}{\sigma_{q+Q}^2}\right) + \log\left(1 + e^{-\left|\frac{4y_{q+Q}}{\sigma_{q+Q}^2}\right|}\right) \tag{2.87}$$

Finally, according to the LLR value, BS decides on the NCS value of qth and $(q+Q)$th transmitted symbol and form NCS vector given in Eq.(2.27) according to the following rule:

$$x_{R_q} = \begin{cases} 1, & \mathrm{LL}_q \geq \mathrm{LL}_{q+Q} \\ -1, & \text{otherwise} \end{cases}, \quad \forall q \in \{1, 2, \cdots, Q\} \tag{2.88}$$

2.3.4. PNC for the users having different SNR values

Up to this section, users are assumed to have the same SNR value, for this section, as a more realistic scenario, the different SNR case, is considered for the estimation of NCS with linear detection schemes.

For this scenario, the received vector $\mathbf{r}$ is given in Eq.(2.17) with different pathloss coefficient for each user. For this section, it is considered that SNR value belonging to kth user γ_k given in Eq.(2.25) is different for each user.

For ZF solution, the inverse of the channel matrix $\hat{\mathbf{G}}_d$ is given in Eq.(2.53).

Theorem 2.3.5 *The equalization matrix for PNC with MMSE for different SNR case $\hat{\mathbf{G}}_d$, is given as following:*

$$\hat{\mathbf{G}}_d = (\hat{\mathbf{H}}_d^H \hat{\mathbf{H}}_d + \frac{1}{2\gamma_0}\mathbf{I}_{L\times L})^{-1}\hat{\mathbf{H}}_d^H \tag{2.89}$$

where $\hat{\mathbf{H}}_d$ is the manipulated composite channel matrix in which the pathloss coefficients are embedded which is given by

$$\hat{\mathbf{H}}_d = \hat{\mathbf{H}}\sqrt{\mathbf{\Gamma}} \tag{2.90}$$

Finally, the steps for the estimation of NCS are equivalent to the steps given in the Section 2.3.3 between Eq.(2.73) and Eq.(2.88).

2.3.5. A Low Complexity for MIMO-PNC

In the previous works, the BS estimates the sum and differences and maps them to NCS by using LLR. In our approach, the sum and difference signals are also used. However, to come up with a low complexity, instead of LLR, the squared differences of the sum and difference signals are used. In Table 2.2, representation of XOR operation of qth and $(q+Q)$th symbol as multiplication operation in signal level can be followed for a reverse mapping of BPSK. Then, we need to analyze that how these squared differences

Table 2.2. XOR Operation in Bit Level, Multiplication in Signal Level

b_q	b_{q+Q}	$b_q \oplus b_{q+Q}$	x_q	x_{q+Q}	$x_{R_q} = x_q x_{q+Q}$
0	0	0	1	1	1
0	1	1	1	-1	-1
1	0	1	-1	1	-1
1	1	0	-1	-1	1

result in multiplication operation which can be derived only by some simple algebraic steps. First, the squared difference of the sum and difference of qth and $(q+Q)$th symbol is taken as:

$$x_{R_q} = (x_q + x_{q+Q})^2 - (x_q - x_{q+Q})^2 \tag{2.91}$$

$\forall q \in \{1, 2, \cdots, Q\}$. After, if we expand the squared terms, x_{R_q} can be revised as:

$$x_{R_q} = x_q^2 + 2x_q x_{q+Q} + x_{q+Q}^2 - (x_q^2 - 2x_q x_{q+Q} + x_{q+Q}^2) \tag{2.92}$$

After the simplifications, the expression for NCS becomes:

$$x_{R_q} = 4x_q x_{q+Q} \tag{2.93}$$

However, the exact value of the sum and difference is not known. Since only y_q and y_{q+Q} are available at BS given in Eq.(2.51), the squared difference of the elements of the equalized vector is taken by the following equation

$$y_{m_q} = y_q^2 - y_{q+Q}^2 \tag{2.94}$$

When, the equalized signals are defined explicitly, y_{m_q} is given as:

$$y_{m_q} = (x_q + x_{q+Q} + n_q)^2 - (x_q - x_{q+Q} + n_{q+Q})^2 \tag{2.95}$$

After some algebraic operations, the expression for y_{m_q} becomes:

$$y_{m_q} = 4x_q x_{q+Q} + 2x_q(n_q - n_{q+Q}) + 2x_{q+Q}(n_q + n_{q+Q}) + (n_q^2 - n_{q+Q}^2) \tag{2.96}$$

If we focus on the multiplication term, the other remaining terms can be merged as a simple noise term which can be denoted as n_{m_q}. Then, the Eq. (2.96) is arranged as:

$$y_{m_q} = 4x_q x_{q+Q} + n_{m_q} \tag{2.97}$$

Finally, each element of NCS vector given in Eq.(2.27) can be estimated by the following equation:

$$x_{R_q} = \begin{cases} 1, & y_{m_q} > 0 \\ -1, & y_{m_q} \leq 0 \end{cases} \tag{2.98}$$

2.4. Performance Evaluations

For this section, firstly, the simulation and theoretical BER performances of PNC, NC and BPSK are provided for single antenna systems. Then, BER performance evaluations are given for multi-user massive MIMO-PNC and multi-user massive MIMO-NC with linear detection. Finally, BER performance of the proposed MIMO-PNC with MMSE technique is given.

In the Figure 2.10, both theoretical and simulation BER performances of PNC, NC and BPSK are given for AWGN channel. A perfect match is observed between theoretical and simulated results. A slight improvement on the BER performance of PNC on NC is shown.

In the Figure 2.11, BER performances of the MIMO, MIMO-PNC and MIMO-NC with ZF and MMSE are given for QPSK modulation. For ZF detector, PNC outperforms NC about 1.5 dB when the BER is less than 10^{-1}. For MMSE detector, PNC outperforms NC about 2.5 dB when the BER is less than 10^{-2}. MMSE outperforms ZF detector for both NC and PNC. It can be also observed that MIMO-PNC outperforms MIMO for both MMSE and ZF.

In the Figures 2.12 and 2.13, BER performances of the multi-user massive MIMO-PNC and multi-user MIMO-NC with ZF and MMSE are given for different M, K and N for QPSK modulation. The simulation results show that as the number of the receiver and transmitter antennas increases MMSE improves performance for both NC and PNC. However, the performance of ZF degrades as the total number of antennas increases for both NC and PNC.

In the Figure 2.14, BER performances of the multi-user massive MIMO, the multi-user massive MIMO-PNC and multi-user massive MIMO-NC with ZF and MMSE are given for $M = 64$, $K = 16$ and $N = 4$ for QPSK modulation. In this Figure, PNC scheme outperforms NC scheme. The performance gain is significant in the high SNR regime, while for the low SNR regime, the performance converges for both ZF and MMSE detection. It can be also observed that multi-user massive MIMO-PNC outperforms multi-user massive MIMO for MMSE and ZF receivers.

In the Figure 2.15, BER performances of the multi-user massive MIMO-PNC and multi-user massive MIMO-NC with ZF and MMSE are given for $M = 120$, $K = 12$

and $N = 10$ for QPSK modulation. In this Figure, it can be again demonstrated that for low SNR regime, the performance of PNC converges to the performance of NC. The significant gain of PNC on NC can be again shown in the high SNR regime.

In the Figures 2.16 and 2.17, BER performances of the MIMO-PNC and MIMO-NC with linear detection are given when SNR values are different for the users for BPSK modulation. It can be showed that for both MMSE and ZF, PNC still outperforms NC as the SNR difference is increased.

In Figure 2.18, it is demonstrated that proposed MIMO-PNC with MMSE scheme gives same performance with MIMO-NC with MMSE while having less complexity compared to LLR based detection.

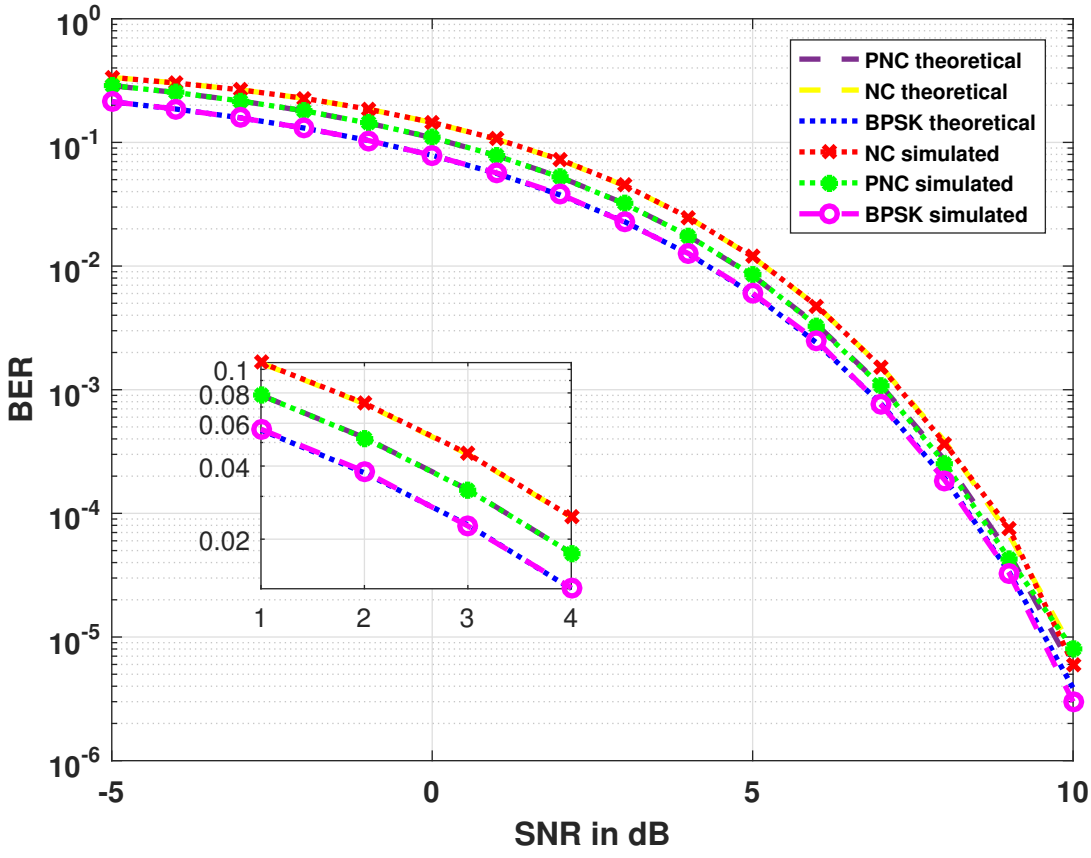

Figure 2.10. Theoretical and simulated BER performances of BPSK, NC and PNC in AWGN channel

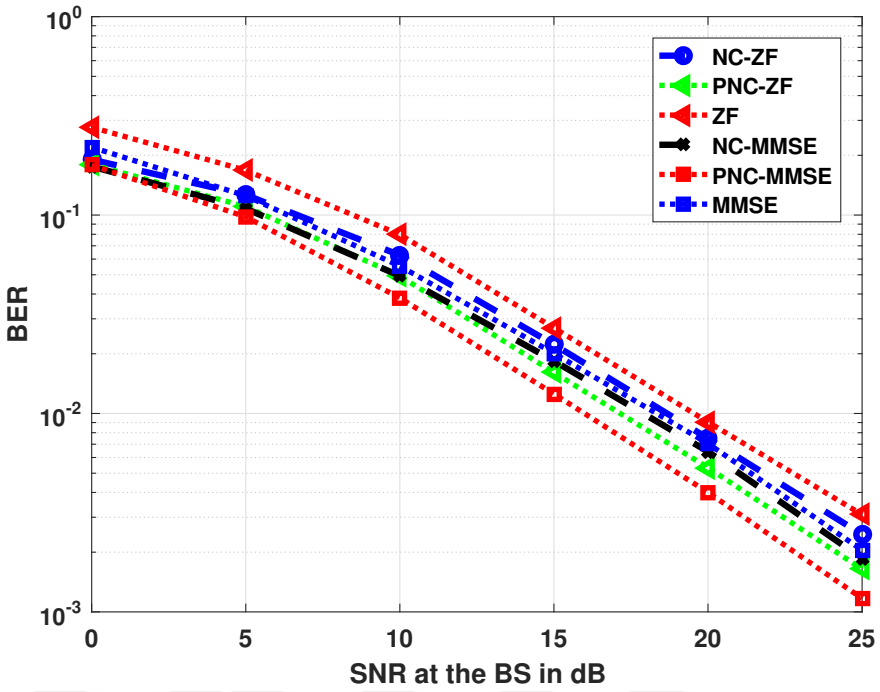

Figure 2.11. BER performances of the MIMO, MIMO-NC and MIMO-PNC with ZF and MMSE with $M = 2, K = 2, N = 1$.

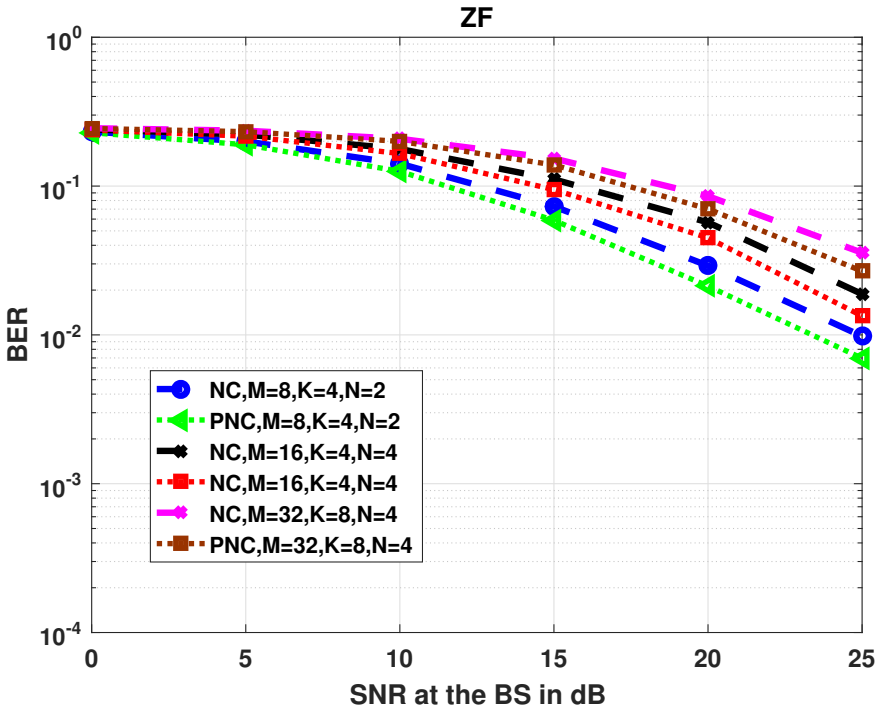

Figure 2.12. BER performances of the multi-user MIMO-NC and multi-user MIMO-PNC with ZF for different M,K and N and QPSK.

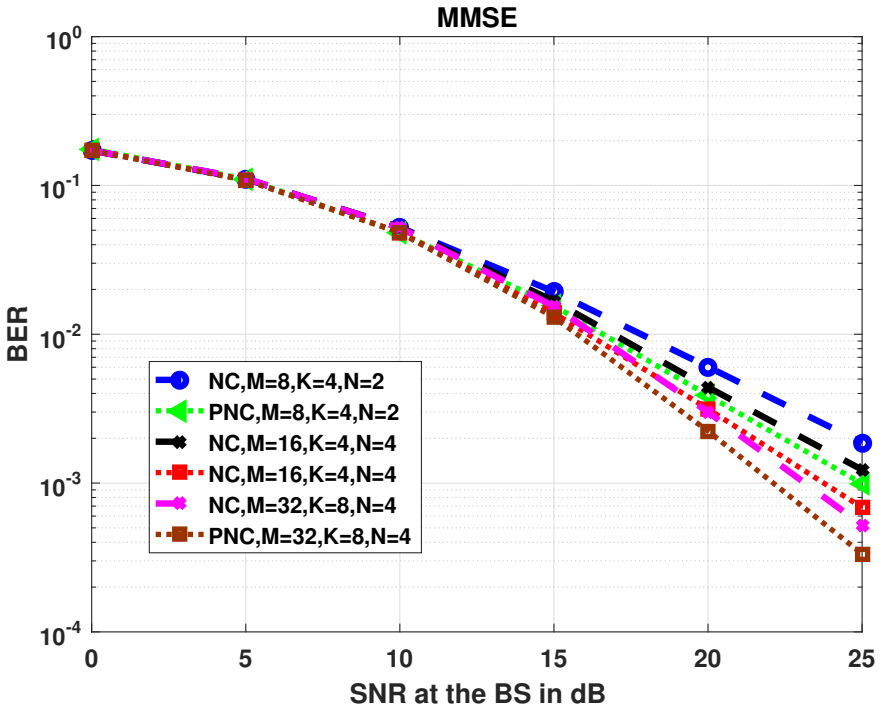

Figure 2.13. BER performances of the multi-user MIMO-NC and multi-user MIMO-PNC with MMSE for different M,K and N and QPSK.

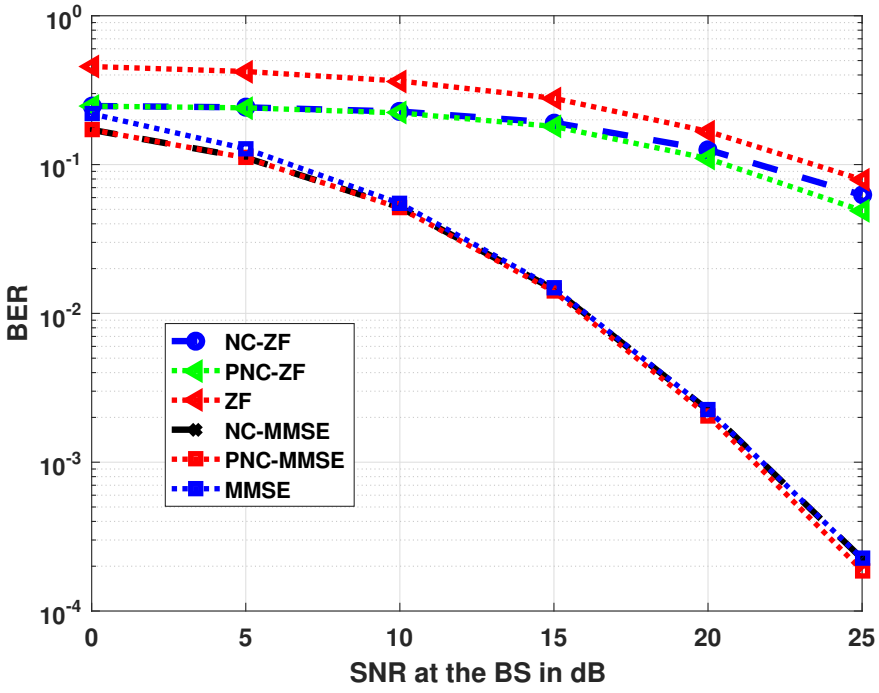

Figure 2.14. BER performances of the multi-user massive MIMO, the multi-user massive MIMO-NC and multi-user massive MIMO-PNC with linear detection with $M = 64, K = 16, N = 4$ and QPSK.

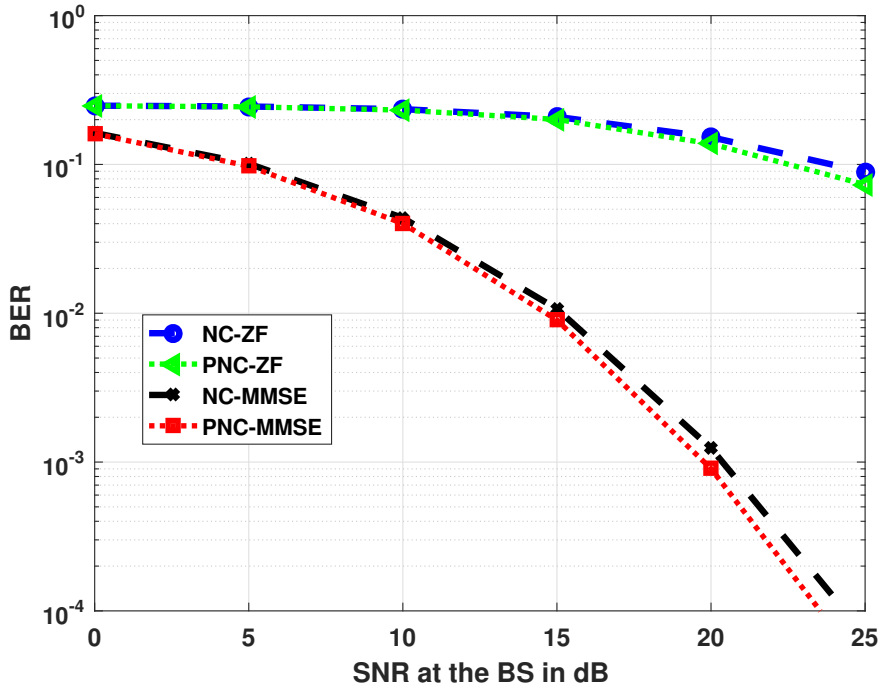

Figure 2.15. BER performances of the multi-user massive MIMO-NC and multi-user massive MIMO-PNC with linear detection with $M = 120, K = 12, N = 10$ and QPSK.

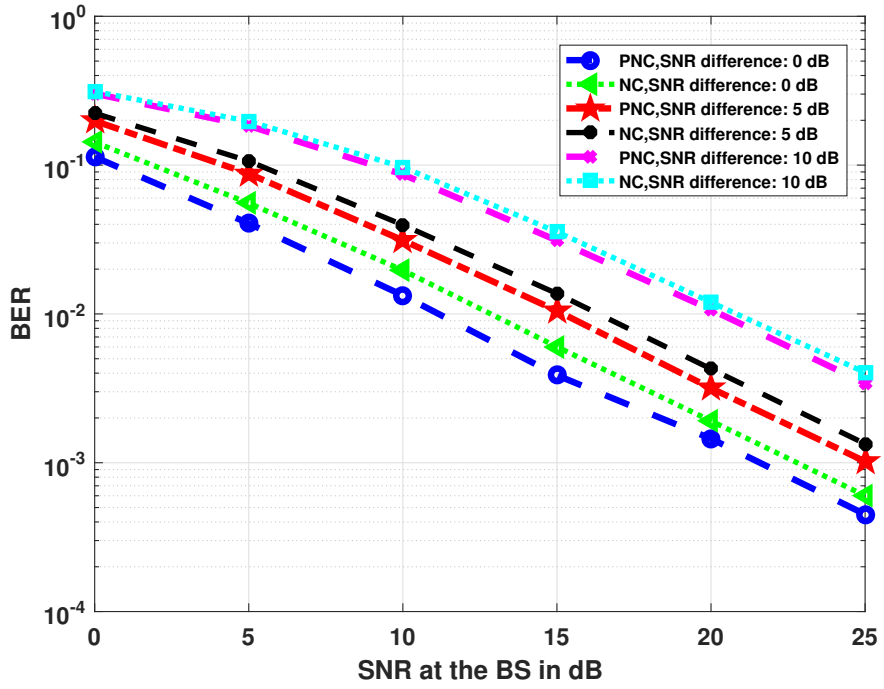

Figure 2.16. BER performances of the MIMO-NC and MIMO-PNC with ZF for different SNR case with $M = 2, K = 2, N = 1$ and BPSK.

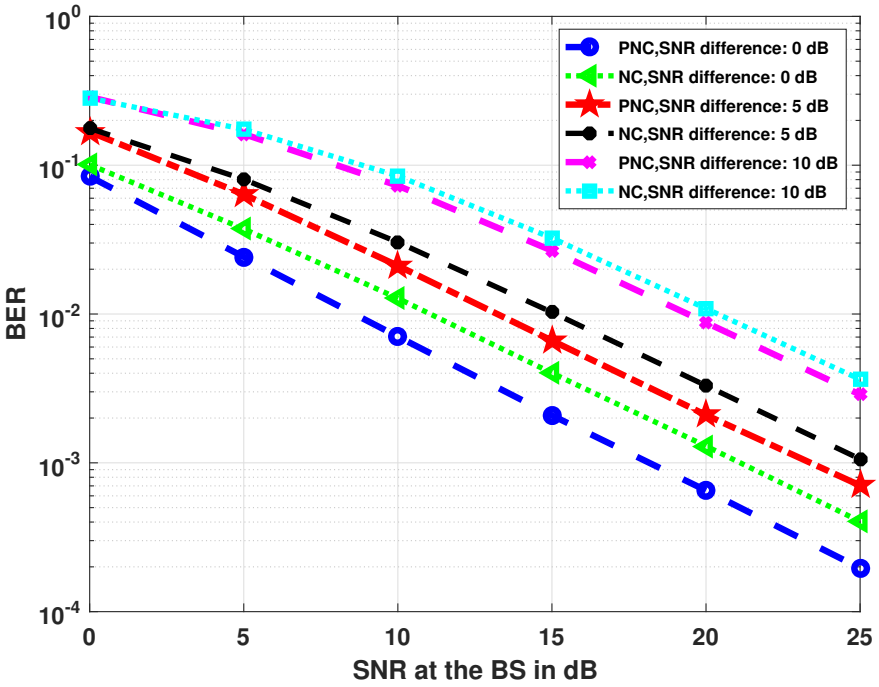

Figure 2.17. BER performances of the MIMO-NC and MIMO-PNC with MMSE for different SNR case with $M = 2, K = 2, N = 1$ and BPSK.

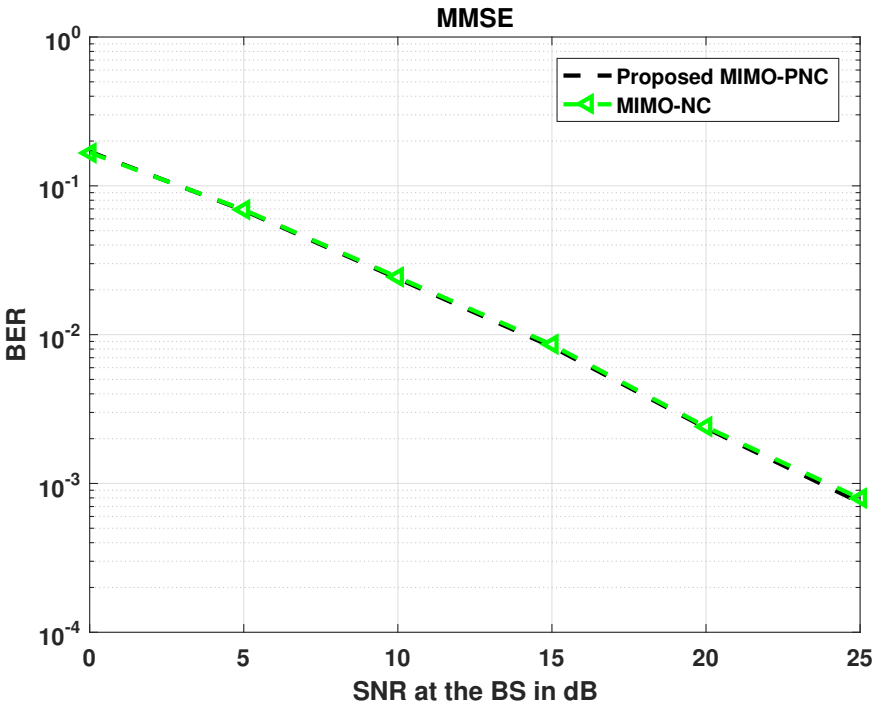

Figure 2.18. BER performances of the MIMO-NC with MMSE and proposed MIMO-PNC with MMSE with $M = 2, K = 2, N = 1$ and BPSK

CHAPTER 3

COVERAGE ANALYSIS OF PHYSICAL LAYER NETWORK CODING

In this chapter, we derive a closed form coverage probability when ZF equalization is used according to the expressions for the distribution of the SNR after equalization for PNC (İlgüy et al., 2020). This chapter is organized as follows: First, the overview of related works are given. Then, the system model is represented. After, the coverage analysis for PNC is represented. Finally, performance evaluations are given.

3.1. Overview

In the literature, for the performance evaluation of PNC, the capacity and BER performances metrics have been used mostly. In (Zhang et al., 2006), the concept of PNC was given where the authors highlighted the performance boost in terms of network capacity provided by PNC. In (Louie et al., 2009), the authors compared the BER and sum data rate performances of PNC with NC and the conventional transmission scheme when the terminal nodes have different SNR values.

Since PNC decides the suitable NCS according to the received constellation, its performance highly depends on the modulation type. In the literature, PNC has been examined through different modulation schemes. In (Lu et al., 2017; Namboodiri et al., 2013; Lu et al., 2009), the authors examined the performances of PNC over different modulation schemes such as QPSK, M-ary phase shift keying (M-PSK) and M-ary quadrature amplitude modulation (M-QAM) based on closed form BER expressions. Since merging MIMO and PNC increases the network performance, in (Zhang and Liew, 2010), the linear equalization techniques for PNC with multiple antennas have been presented. The focus on this approach is to estimate the NCS in the MAC phase by using the sum and difference of the baseband signals coming from the different UEs. These signals are estimated with the help of an equalization process in which the sum-difference matrix is

embedded. The equalization matrix has been determined by using zero ZF and MMSE techniques. After the equalization process, an estimate of a vector which consists of the sum and difference baseband signals is obtained. These estimates are used to form the LLR of the NCS, where the LLR consists of the information about the variances on each antenna after the equalization. Assuming the availability of perfect CSI at the BS, the covariance matrix of the equalized noise can be easily estimated with help of the inverse channel matrices. In (Kumar et al., 2019; Li et al., 2013; Okyere et al., 2019), the MIMO-PNC systems have been examined by considering vertical Bell Labs Space Time (V-BLAST) detection, user-antenna selection and multi user communication.

The coverage analysis of the MIMO systems without considering PNC has been studied in (Razeghi et al., 2014; Kumar et al., 2015; Khoshkholgh et al., 2017). Besides, the cellular network analysis based on stochastic geometry have been presented to evaluate coverage in (Andrews et al., 2016; Parida and Dhillon, 2019; Null et al., 2014). For stochastic geometry-based cellular network, the signal-to-interference-plus-noise ratio (SINR) distribution is computed to characterize the coverage probability for the single antenna case in (Andrews et al., 2016) while the MIMO systems have been covered by (Parida and Dhillon, 2019; Null et al., 2014). Further, the coverage and outage analysis for cellular networks have been presented in (Monhof et al., 2018; Panziyu and Baoziyong, 2018) considering secrecy and heterogeneity. For the PNC with single antenna case, the coverage probability analysis has been given in (Fukui et al., 2014). In this chapter, we derive the closed form expression of coverage probability for the massive MIMO-PNC by using linear equalization techniques, which has not been covered by the literature to the best knowledge of the authors.

3.2. System Model

The system model consists of one BS equipped with M antennas and K UEs equipped with a single antenna ($N = 1$) given in Figure 3.1. All users have the same SNR value and each user has a pair to communicate with BPSK modulation. The users and BS are synchronized and all users send their data simultaneously to the BS. The received vector $\mathbf{r}$ is given in Eq.(2.17), for $Q = K/2, L = K$. Before starting the coverage probability analysis we give the expression for the SNR after equalization.

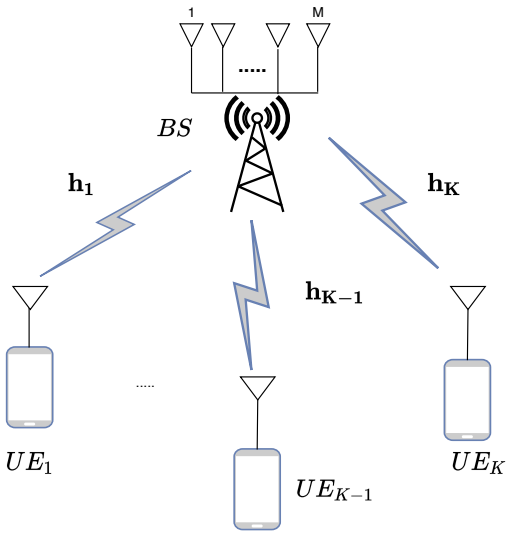

Figure 3.1. System Model for multi-user SIMO-PNC

Theorem 3.2.1 *SNR after equalization for kth estimated symbol for PNC ρ_k is defined as follows:*

$$\rho_k = \frac{2\gamma_0}{\{(\hat{\mathbf{H}}^H\hat{\mathbf{H}})^{-1}\}_{k,k}}, \quad \forall k \in \{1, 2, \cdots, K\} \tag{3.1}$$

where the received SNR at the BS per antenna γ_0 is defined in Eq.(2.26) and manipulated channel matrix $\hat{\mathbf{H}}$ is given in Eq.(2.47).

Proof

By using the expression of the equalized signal in Eq.(2.51) and knowing that $\mathbb{E}\{||\hat{\mathbf{G}}\hat{\mathbf{H}}||_{\mathbf{F}}^{\mathbf{2}}\} = M$, the SNR after equalization for kth estimated symbol can be defined as follows: SNR term after equalization for kth estimated symbol can be defined as follows:

$$\rho_k = \frac{M[\mathbb{E}\{\hat{\mathbf{x}}\hat{\mathbf{x}}^H\}]_{k,k}}{[\mathrm{E}\{\hat{\mathbf{G}}\mathbf{n}\mathbf{n}^H\hat{\mathbf{G}}^H|\mathbf{H}\}]_{k,k}} \tag{3.2}$$

Then, Eq.(2.48) is used to express $\hat{\mathbf{x}}$ explicitly in Eq.(3.2) as follows:

$$\rho_k = \frac{M[\mathbb{E}\{\mathbf{D}\mathbf{x}\mathbf{x}^H\mathbf{D}\}]_{k,k}}{[\mathrm{E}\{\hat{\mathbf{G}}\mathbf{n}\mathbf{n}^H\hat{\mathbf{G}}^H|\mathbf{H}\}]_{k,k}} \tag{3.3}$$

Since $\mathbf{D}$ is a deterministic matrix in Eq.(3.3), it can be taken out from the expectation operator as follows:

$$\rho_k = \frac{M[\mathbf{D}\mathbb{E}\{\mathbf{x}\mathbf{x}^H\}\mathbf{D}^H]_{k,k}}{[\mathrm{E}\{\hat{\mathbf{G}}\mathbf{n}\mathbf{n}^H\hat{\mathbf{G}}^H|\mathbf{H}\}]_{k,k}} \tag{3.4}$$

By using the auto covariance matrix of the transmit symbol given in Eq.(2.23), the numerator of Eq.(3.4) is revised as follows:

$$\rho_k = \frac{M\dfrac{\mathrm{P}}{K}[\mathbf{D}\mathbf{I}\mathbf{D}^H]_{k,k}}{[\mathrm{E}\{\hat{\mathbf{G}}\mathbf{n}\mathbf{n}^H\hat{\mathbf{G}}^H|\mathbf{H}\}]_{k,k}} \tag{3.5}$$

Since $\mathbf{D}\mathbf{D}^H = 2\mathbf{I}$, the final expression for the numerator of Eq.(3.5) is obtained as $\dfrac{2\mathrm{MP}}{K}$ which is given as follows:

$$\rho_k = \frac{\dfrac{2\mathrm{MP}}{K}}{[\mathrm{E}\{\hat{\mathbf{G}}\mathbf{n}\mathbf{n}^H\hat{\mathbf{G}}^H|\mathbf{H}\}]_{k,k}} \tag{3.6}$$

Knowing that the conditional expectation conditioning on $\mathbf{H}$ is taken, $\hat{\mathbf{G}}$ is not random for this expectation and can be taken out from the expectation operator for Eq.(3.6) as follows:

$$\rho_k = \frac{\dfrac{2\mathrm{MP}}{K}}{[\hat{\mathbf{G}}\mathrm{E}\{\mathbf{n}\mathbf{n}^H\}\hat{\mathbf{G}}^H]_{k,k}} \tag{3.7}$$

After the replacement of the auto covariance matrix of the noise vector $\sigma_n^2\mathbf{I}_{M\times M}$, Eq.(3.7) becomes:

$$\rho_k = \frac{\dfrac{2\mathrm{MP}}{K}}{\sigma_n^2[\hat{\mathbf{G}}\hat{\mathbf{G}}^H]_{k,k}} \tag{3.8}$$

Finally, knowing that $\hat{\mathbf{G}}\hat{\mathbf{G}}^H = (\hat{\mathbf{H}}^H\hat{\mathbf{H}})^{-1}$, the expression for ρ_k in Eq.(3.8) is obtained by using Eq.(2.26) as follows:

$$\rho_k = \frac{2\gamma_0}{[(\hat{\mathbf{H}}^H\hat{\mathbf{H}})^{-1}]_{k,k}} \tag{3.9}$$

End of the Proof

3.3. Coverage Probability of MIMO-PNC

In this section, based on the SNR value after equalization in Eq.(3.1), the coverage probability for a user pair is defined. The coverage probability of PNC for a user pair is the probability that minimum SNR value after equalization of qth and $(q+Q)$th users are greater than a threshold τ.

$$\mathrm{p}^{cov}(\tau) = \Pr(\min(\rho_q, \rho_{q+Q}) \geq \tau), \quad \forall q \in \{1, 2, \cdots, Q\} \tag{3.10}$$

Hence, for Eq.(3.10), the probability that minimum of two random variable is greater than a value can be expressed by the joint probabilities of two events which is given below:

$$\mathrm{p}^{cov}(\tau) = \Pr(\rho_q \geq \tau, \rho_{q+Q} \geq \tau) \tag{3.11}$$

Since two events in Eq.(3.11) are independent from each other, the coverage probability can be defined as the multiplication of the separate events as:

$$\mathrm{p}^{cov}(\tau) = \Pr(\rho_q \geq \tau)\Pr(\rho_{q+Q} \geq \tau) \tag{3.12}$$

Further, since the coverage probability of PNC is defined, to derive a closed form, the probability density function (PDF) of the SNR after equalization is needed.

Theorem 3.3.1 *The SNR value after ZF equalization with sum difference matrix is gamma distributed whose PDF is represented as:*

$$f_{\mathrm{P}_k}(\rho_k) = \frac{1}{\gamma_0(M-K)!}\mathrm{e}^{\left(-\frac{\rho_k}{\gamma_0}\right)}\left(\frac{\rho_k}{\gamma_0}\right)^{M-K} \tag{3.13}$$

Proof

(Gore et al., 2002), state that $2\mathbf{H}^H\mathbf{H}$ term is complex Wishart matrix. Then, we can define also a complex Wishart matrix $\hat{\mathbf{Z}}$ formed by the manipulated channel matrix in Eq.(2.47) as $\hat{\mathbf{Z}} = 2\hat{\mathbf{H}}^H\hat{\mathbf{H}}$. Then, the distribution of $\hat{\mathbf{Z}}$ can be described as follows:

$$\mathbf{W}_M(K, \hat{\mathbf{\Sigma}}) = \frac{\mathrm{e}^{\mathrm{tr}(-\hat{\mathbf{\Sigma}}^{-1}\hat{\mathbf{Z}})}|\hat{\mathbf{Z}}|^{(M-K)}}{\Gamma_M(K)|\hat{\mathbf{\Sigma}}|^M} \tag{3.14}$$

where $\hat{\mathbf{\Sigma}}$ is the scale matrix of $\hat{\mathbf{Z}}$ and $\Gamma_M(.)$ is the $M-$variate complex multivariate gamma function. Next, the Eq.(3.1) can be arranged as follows:

$$\rho_k = \gamma_0 \frac{1}{[(\hat{\mathbf{Z}})^{-1}]_{k,k}} \tag{3.15}$$

Further, Eq.(3.15) is rewritten by the inverse matrix definition as follows:

$$\rho_k = \gamma_0 \frac{|\hat{\mathbf{Z}}|}{|\hat{\mathbf{Z}}_{k,k}|}. \tag{3.16}$$

Next, the fact $|\hat{\mathbf{Z}}| = |\hat{\mathbf{Z}}_{k,k}||\hat{\mathbf{Z}}^{sc}_{k,k}|$ is used to achieve $\rho_k = \gamma_0|\hat{\mathbf{Z}}^{sc}_{k,k}|$. $\hat{\mathbf{Z}}^{sc}_{k,k}$ can be also defined as a Wishart matrix distributed as $\mathbf{W}_1(M-K+1, \hat{\mathbf{\Sigma}}^{sc}_{kk})$. In other word, $\mathrm{s} = |\hat{\mathbf{Z}}^{sc}_{k,k}|$ is a Chi squared random variable where its PDF is given below:

$$f_{\mathrm{S}}(\mathrm{s}) = \frac{\mathrm{e}^{-\frac{\mathrm{s}}{\hat{\mathbf{\Sigma}}^{sc}_{kk}}}}{\hat{\mathbf{\Sigma}}^{sc}_{kk}(M-K)!}\left(\frac{\mathrm{s}}{\hat{\mathbf{\Sigma}}^{sc}_{kk}}\right)^{M-K} \tag{3.17}$$

After, the following change of variable is held to find the PDF of ρ_k as $\mathrm{s} = |\hat{\mathbf{Z}}^{sc}_{k,k}| = \dfrac{\rho_k}{\gamma_0}$. Since Schur complement of the minor is a scalar, its determinant becomes itself $\mathrm{s} = \hat{\mathbf{Z}}^{sc}_{k,k} = \dfrac{\rho_k}{\gamma_0}$. Because change of variable to Chi squared variable s is made, its corresponding scale matrix must be changed from $\hat{\mathbf{\Sigma}}^{sc}_{kk}$ to $\gamma_0\hat{\mathbf{\Sigma}}^{sc}_{kk}$. Then, Eq.(3.17) becomes:

$$f_{\mathrm{S}}\left(\frac{\rho_k}{\gamma_0}\right) = \frac{\mathrm{e}^{-\dfrac{\rho_k}{\gamma_0^2\hat{\mathbf{\Sigma}}^{sc}_{kk}}}}{\gamma_0\hat{\mathbf{\Sigma}}^{sc}_{kk}(M-K)!}\left(\frac{\rho_k}{\gamma_0^2\hat{\mathbf{\Sigma}}^{sc}_{kk}}\right)^{(M-K)} \tag{3.18}$$

Since in the argument of the function above, we have $\dfrac{\rho_k}{\gamma_0}$, this function in Eq.(3.18) does not stands for the PDF of ρ_k. In order to obtain PDF, ρ_k must be replaced with $\rho_k\gamma_0$ as follows:

$$f_{\mathrm{P}_k}(\rho_k) = \frac{\mathrm{e}^{-\dfrac{\rho_k}{\gamma_0\hat{\mathbf{\Sigma}}^{sc}_{kk}}}}{\gamma_0\hat{\mathbf{\Sigma}}^{sc}_{kk}(M-K)!}\left(\frac{\rho_k}{\gamma_0\hat{\mathbf{\Sigma}}^{sc}_{kk}}\right)^{(M-K)} \tag{3.19}$$

Since $\hat{\mathbf{\Sigma}}^{sc}_{kk} = \dfrac{1}{[(\hat{\mathbf{\Sigma}})^{-1}]_{kk}}$ and knowing that the first moment of a Wishart matrix $\hat{\mathbf{Z}}$ is the multiplication of its scale matrix $\hat{\mathbf{\Sigma}}$ with its degree of the freedom M, the scale matrix can be obtained by the following equation:

$$\hat{\mathbf{\Sigma}} = \frac{1}{M}\mathbb{E}\{\hat{\mathbf{Z}}\} = \frac{2}{M}\mathbb{E}\{\hat{\mathbf{H}}^H\hat{\mathbf{H}}\} \tag{3.20}$$

By the Eq.(2.47), the expression for the scale matrix in Eq.(3.20) becomes:

$$\hat{\mathbf{\Sigma}} = \frac{2}{M}\mathbf{D}^{-1}\mathbb{E}\{\mathbf{H}^H\mathbf{H}\}\mathbf{D}^{-1} \tag{3.21}$$

Since, $\mathbb{E}\{\mathbf{H}^H\mathbf{H}\} = M\mathbf{I}$ by Eq.(2.19) and $\mathbf{D}^{-2} = \dfrac{1}{2}\mathbf{I}$, the scale matrix can be obtained as $\hat{\mathbf{\Sigma}} = \mathbf{I}$ which gives $\hat{\mathbf{\Sigma}}^{sc}_{kk} = 1$. After the replacement of $\hat{\mathbf{\Sigma}}^{sc}_{kk}$ into Eq.(3.19), Eq.(3.13) is obtained as follows:

$$f_{\mathrm{P}_k}(\rho_k) = \frac{1}{\gamma_0 (M-K)!} \mathrm{e}^{\left(-\frac{\rho_k}{\gamma_0}\right)} \left(\frac{\rho_k}{\gamma_0}\right)^{M-K} \tag{3.22}$$

End of the proof

After, let define the rate parameter as $\beta = \dfrac{1}{\gamma_0}$. Next, let define the shape parameter as $\alpha = M - K + 1$. After the definition of these parameters, Eq.(3.13) can be rewritten following by:

$$f_{\mathrm{P}_k}(\rho_k) = \frac{\beta^{\alpha}}{\Gamma(\alpha)} \mathrm{e}^{-(\beta\rho_k)} \rho_k^{\alpha-1} \quad \forall k \in \{1, 2, \cdots, 2Q\} \tag{3.23}$$

where $\Gamma(.)$ is the gamma function which is defined as follows:

$$\Gamma(\alpha) = \int_0^{\infty} x^{\alpha-1} e^{-x} dx \tag{3.24}$$

Then, Eq.(3.12) can be rewritten by:

$$\mathrm{p}^{cov}(\tau) = \int_{\tau}^{\infty} f_{\mathrm{P}_q}(\rho_q) d\rho_q \int_{\tau}^{\infty} f_{\mathrm{P}_{q+Q}}(\rho_{q+Q}) d\rho_{q+Q}, \quad \forall q \in \{1, 2, \cdots, Q\} \tag{3.25}$$

In order to achieve the closed form of the coverage probability, the integral terms in Eq.(3.25) can be replaced with the complementary cumulative distribution function (CCDF) of the SNR values after the equalization by the following equation:

$$\mathrm{p}^{cov}(\tau) = (1 - \mathrm{F}_{\rho_q}(\tau))(1 - \mathrm{F}_{\rho_{q+Q}}(\tau)) \tag{3.26}$$

where $\mathrm{F}_{\mathrm{P}_k}$ is the cumulative distribution function (CDF) of the SNR value after equalization which can be represented as:

$$\mathrm{F}_{\mathrm{P}_k}(\rho_k) = \int_0^{\rho_k} f_{\mathrm{P}_k}(u; \beta, \alpha) du = \frac{\gamma(\alpha, \beta\rho_k)}{\Gamma(\alpha)} \tag{3.27}$$

where $\gamma(\alpha, \beta\rho_k)$ is the lower incomplete gamma function as followed by:

$$\gamma(\alpha, \beta\rho_k) = \int_0^{\beta\rho_k} t^{\alpha-1} \mathrm{e}^t dt \tag{3.28}$$

Since, for both qth and $(q+Q)$th equalized SNR value, the parameters β and α for CDF calculation are common, the coverage probability of the PNC for a user pair $\mathrm{p}^{cov}(\tau)$ in Eq.(3.26) becomes:

$$\mathrm{p}^{cov}(\tau) = \left(1 - \frac{\gamma(\alpha, \beta\tau)}{\Gamma(\alpha)}\right)^2 \tag{3.29}$$

Finally, the average coverage probability of PNC for Q user pairs is calculated as follows:

$$\overline{\mathrm{p}^{cov}} = \frac{1}{Q} \sum_{q=1}^{Q} \mathrm{p}^{cov}(\tau) \tag{3.30}$$

3.4. Performance Evaluations

In this section, we illustrate the theoretical and simulation results for different number of antennas and users in the multi-user single input multiple output physical layer network coding (SIMO-PNC) systems with the deployment of moderate to massive number of antennas at the BS. While providing the simulation results, for each iteration, the SNR values after equalization are determined as in Eq.(3.1) based on the composite channel matrix generated through Rayleigh distribution. Then, the lower output SNR value is compared to a given target SNR value. Then, we define a counter which is firstly equal to zero and increased when lower output SNR value is higher than the target SNR value. Finally, in order to find the average coverage probability of user pairs for a target SNR value, the counter value is divided to the number of the iteration and the number of the user pairs. For the theoretical results, the coverage probability for one user pair is directly calculated by using Eq.(3.29) based on the received SNR at the BS per antenna γ_0, the

given target SNR value τ, the number of users K, and the number of the antennas at the BS, M. Then, the average coverage probability for Q user pairs is calculated by using Eq.(3.30)

For the Figures 3.2 and 3.3 theoretical and simulated results for average coverage probability for each user pair are given for $K = 2$ with a received SNR 10 dB and 20 dB respectively. For the Figures 3.4 and 3.5 theoretical and simulated results for average coverage probability for each user pair are given for $K = 4$ with a received SNR 10 dB and 20 dB respectively. For the Figures 3.8 and 3.9 theoretical and simulated results for average coverage probability for each user pair are given for $K = 20$ with a received SNR 10 dB and 20 dB respectively. Thereby, for fixed K, as the number of antennas at BS increases, the system gives better performance.

For the Figures 3.12 and 3.13 theoretical and simulated results for average coverage probability for each user pair are given for a fix $M = 100$ with a received SNR 10 dB and 20 dB respectively. It can be observed that for fixed M, the system performance degrades as the number of the user increases.

In the Figures 3.6, 3.7, 3.10 and 3.11, the theoretical and simulation results of the coverage probability are demonstrated by considering low user SNR values as 0dB and 5dB, respectively for fixed number of user $K = 20$ and fixed number of the antennas in BS. In these Figures, the applicability of PNC-MIMO systems is also demonstrated in the low SNR regimes while preserving the same SNR improvement as in the high SNR regimes.

For the Figures 3.14 and 3.15, average coverage probability per user pair for multi-user SIMO-PNC with ZF when the received SNR is uniformly distributed between 0 and 20 dB for both fixed K and fixed M.

For all results, it can be concluded that the simulation and theoretical results are perfectly matched and it can be also concluded that even the average received is less than a target SNR value, BS can cover the estimation of NCS of the user pairs due to the performance enhancement properties of the MIMO-PNC. For example, for the Figure 3.9, with $M = 30$, for 20 dB received SNR, even the target SNR value is 25 dB, BS can cover 100 percent of the users.

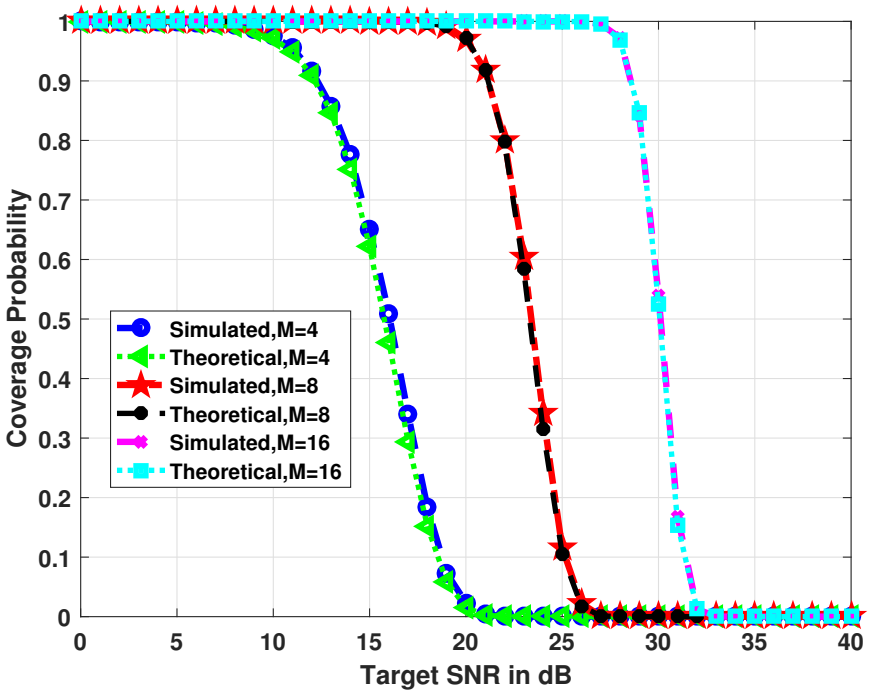

Figure 3.2. Average coverage probability for multi-user SIMO-PNC with $K = 2$, $\gamma_0 = 10$ dB.

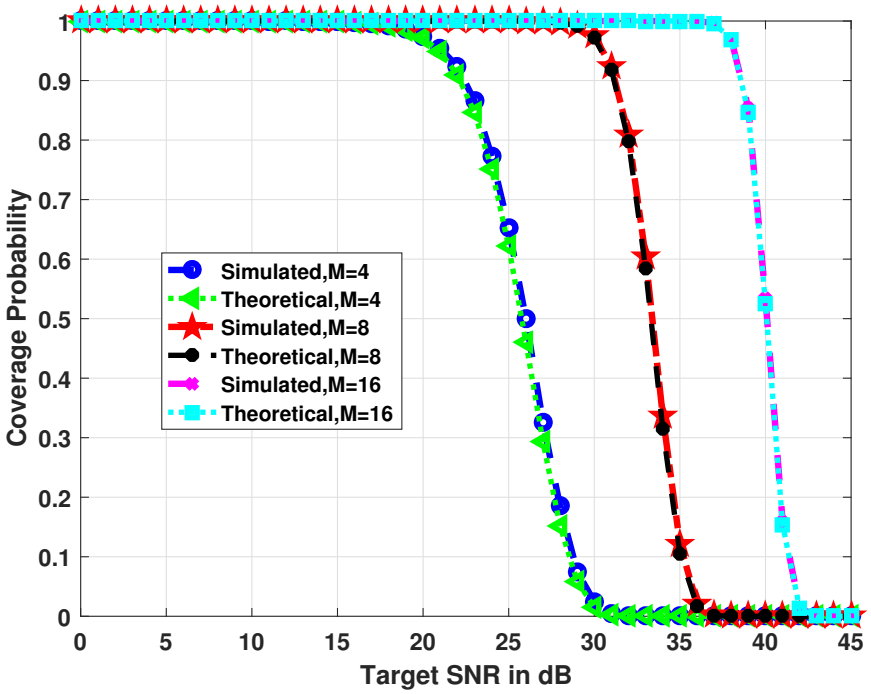

Figure 3.3. Average coverage probability for multi-user SIMO-PNC with $K = 2$, $\gamma_0 = 20$ dB.

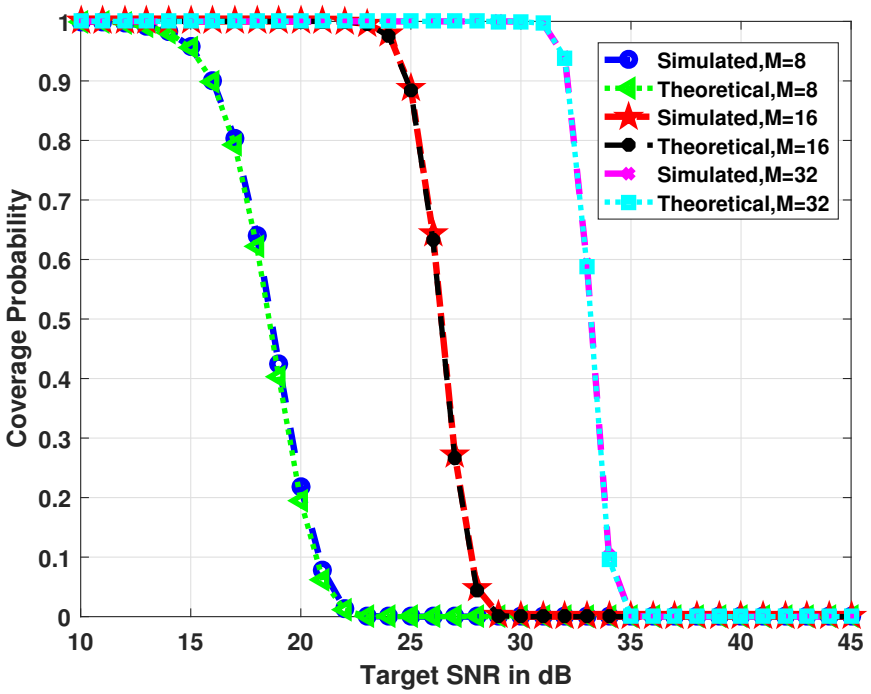

Figure 3.4. Average coverage probability for multi-user SIMO-PNC with $K = 4$, $\gamma_0 = 10$ dB.

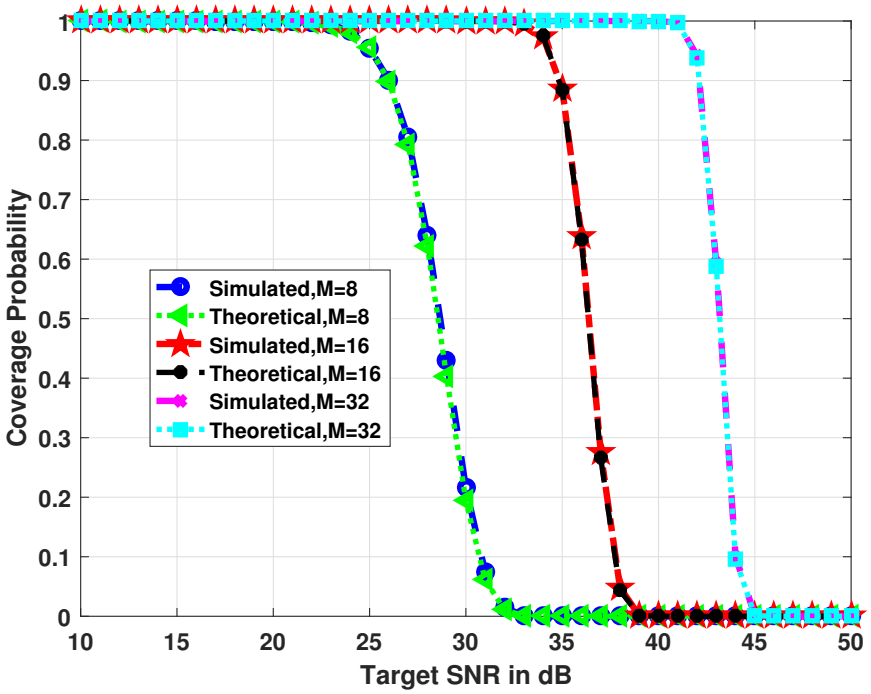

Figure 3.5. Average coverage probability for multi-user SIMO-PNC with $K = 4$, $\gamma_0 = 20$ dB.

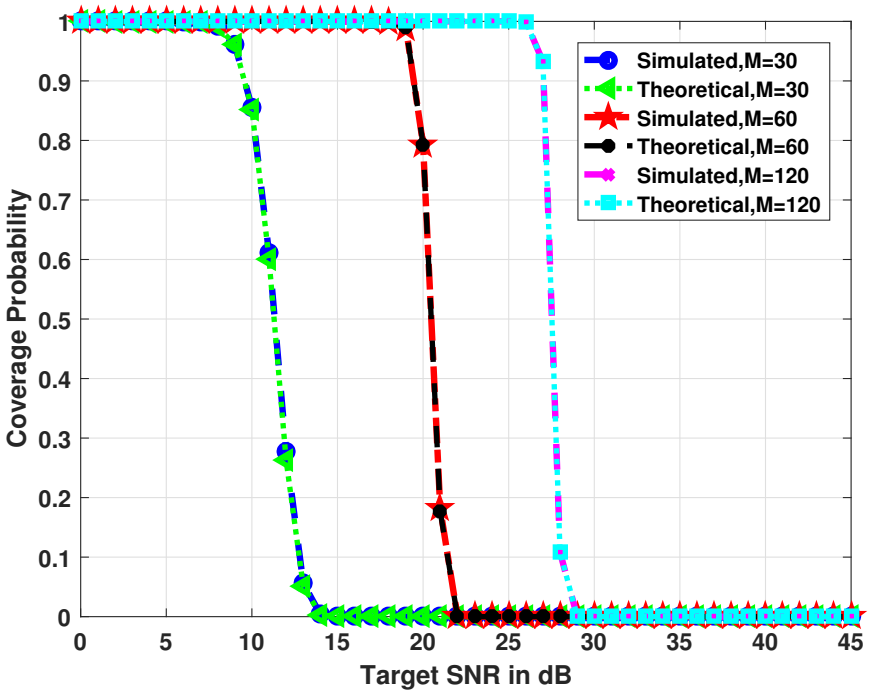

Figure 3.6. Average coverage probability for multi-user SIMO-PNC with $K = 20$, $\gamma_0 = 0$ dB.

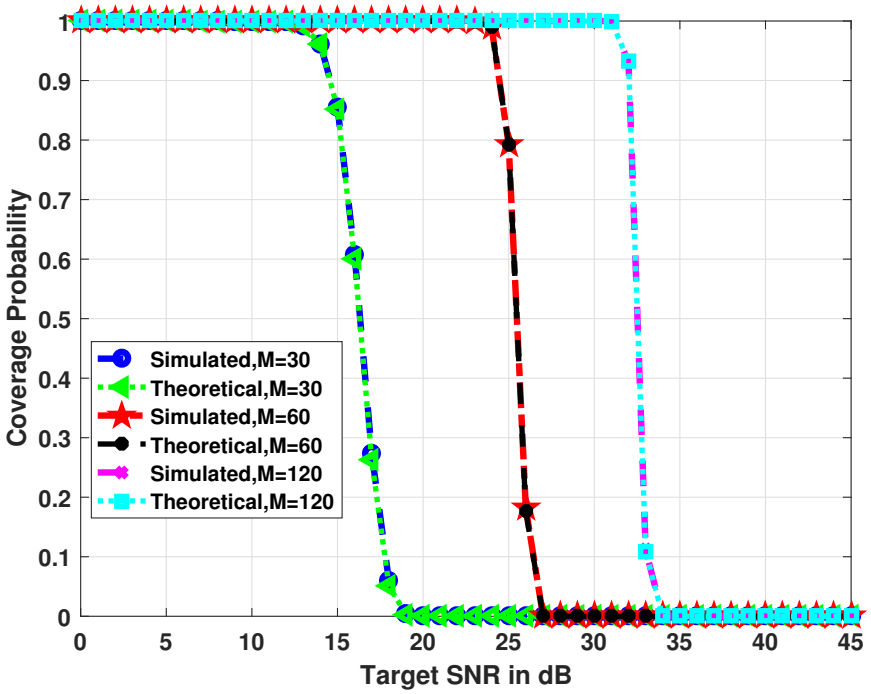

Figure 3.7. Average coverage probability for multi-user SIMO-PNC with $K = 20$, $\gamma_0 = 5$ dB.

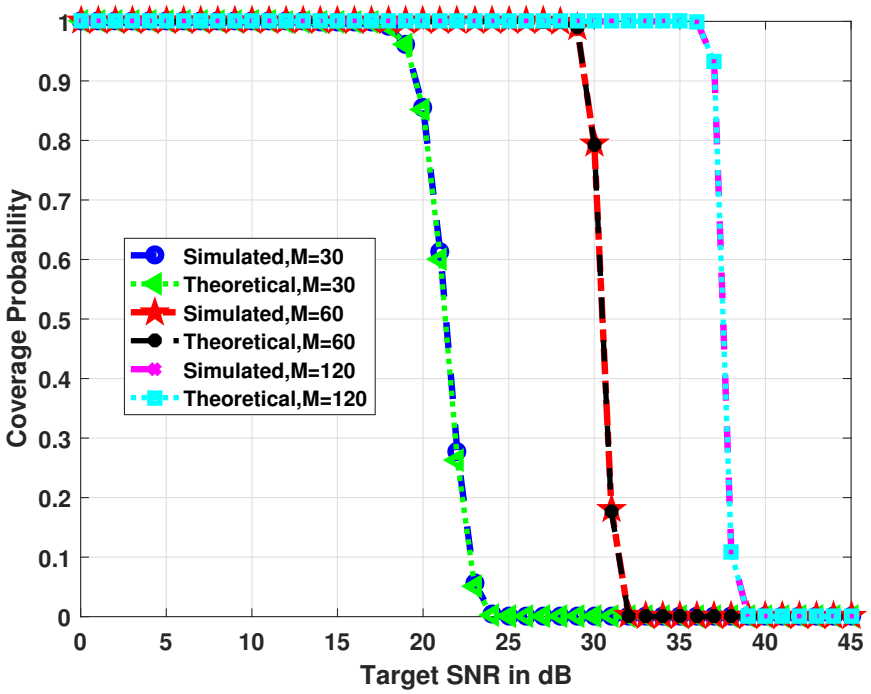

Figure 3.8. Average coverage probability for multi-user SIMO-PNC with $K = 20$, $\gamma_0 = 10$ dB.

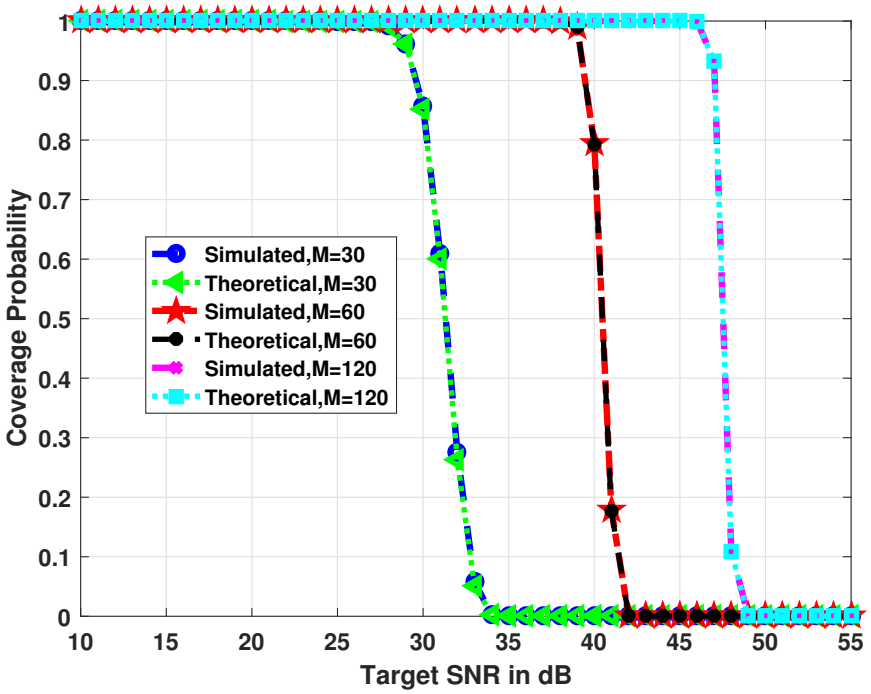

Figure 3.9. Average coverage probability for multi-user SIMO-PNC with $K = 20$, $\gamma_0 = 20$ dB.

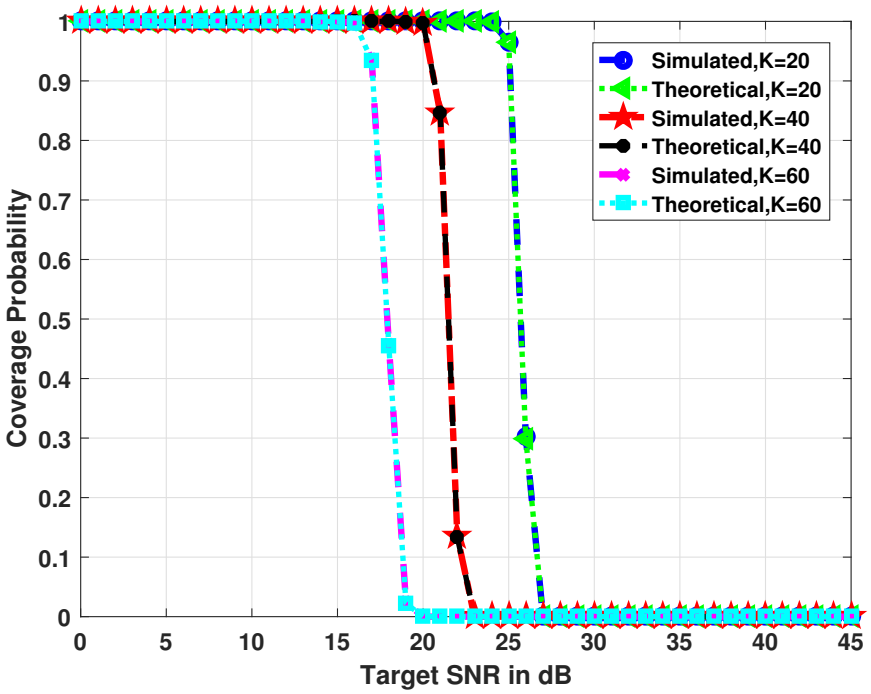

Figure 3.10. Average coverage probability for multi-user SIMO-PNC with $M = 100$, $\gamma_0 = 0$ dB.

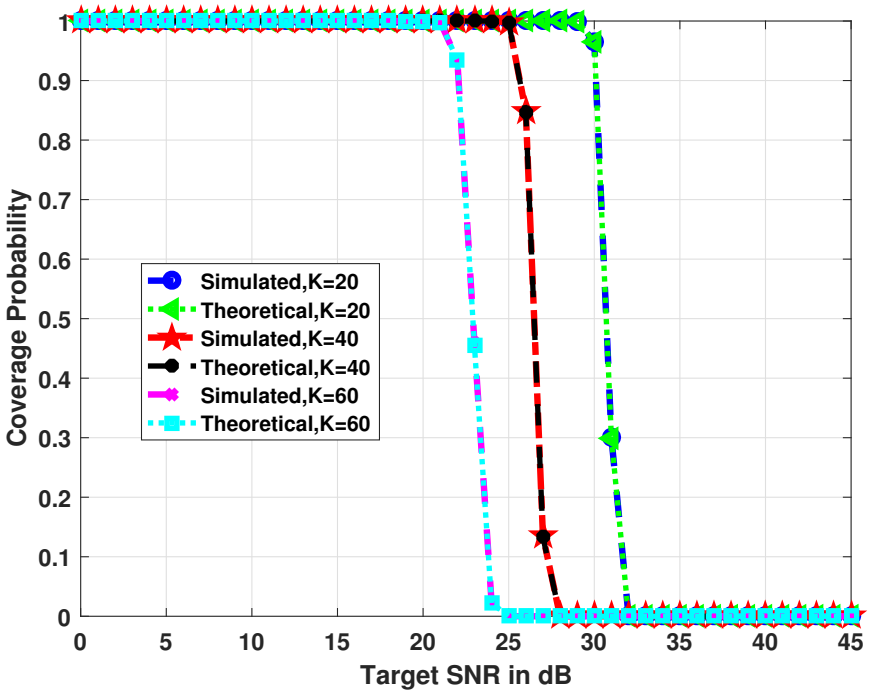

Figure 3.11. Average coverage probability for multi-user SIMO-PNC with $M = 100$, $\gamma_0 = 5$ dB.

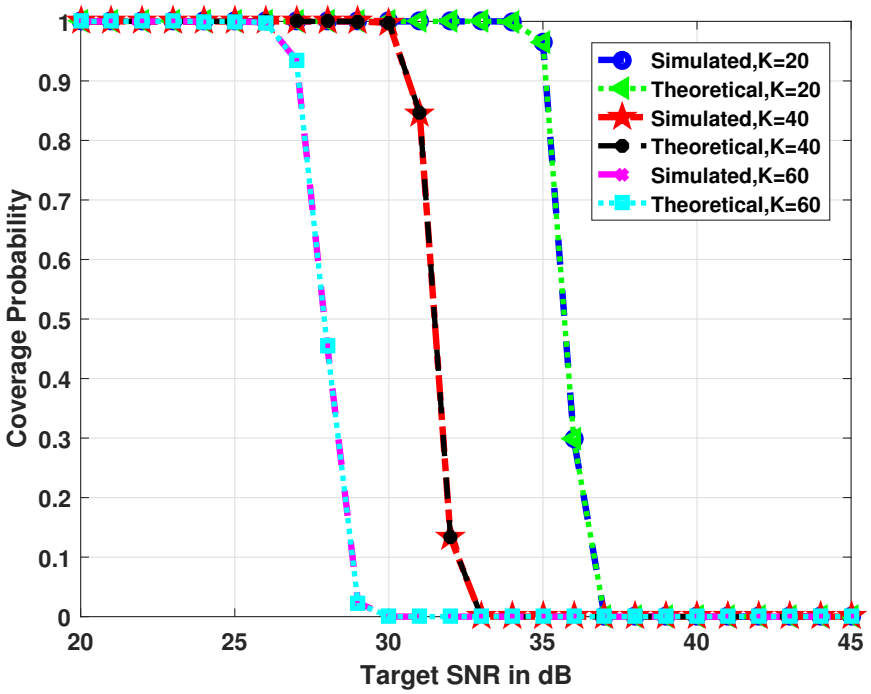

Figure 3.12. Average coverage probability for multi-user SIMO-PNC with $M = 100$, $\gamma_0 = 10$ dB.

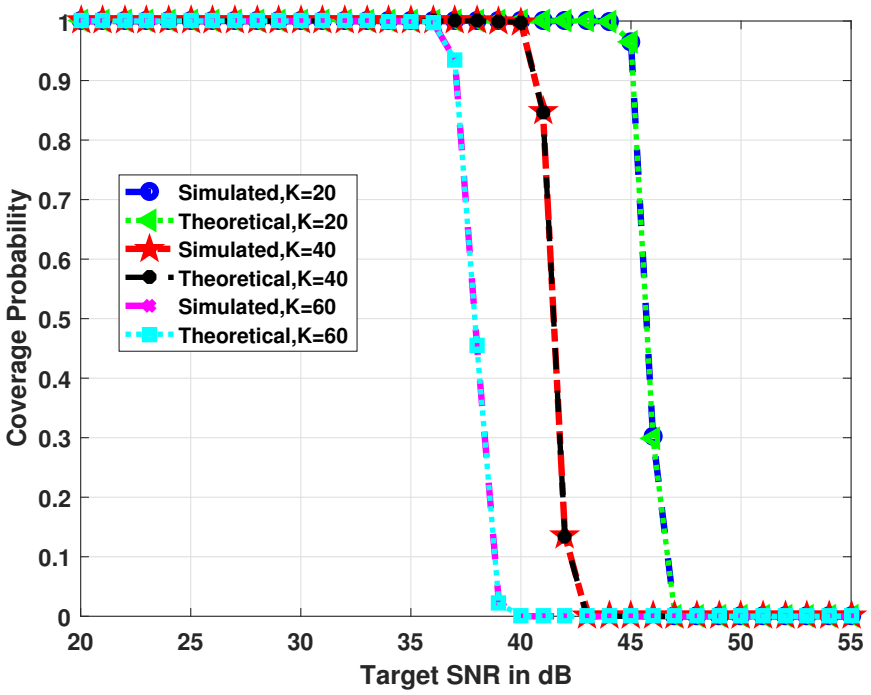

Figure 3.13. Average coverage probability for multi-user SIMO-PNC with $M = 100$, $\gamma_0 = 20$ dB.

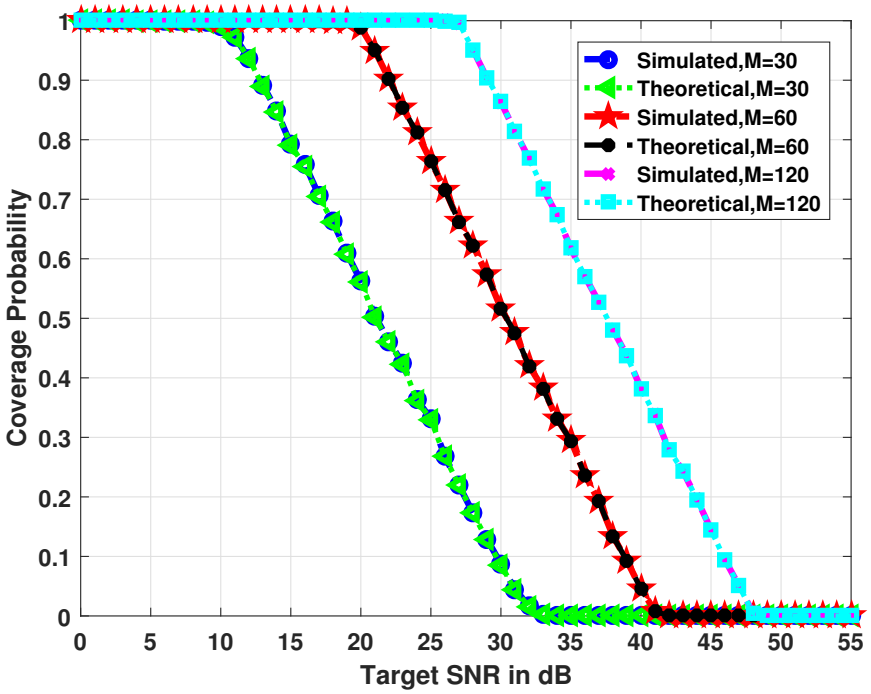

Figure 3.14. Average coverage probability for multi-user SIMO-PNC with $K = 20$ when the received SNR is uniformly distributed between 0 and 20 dB.

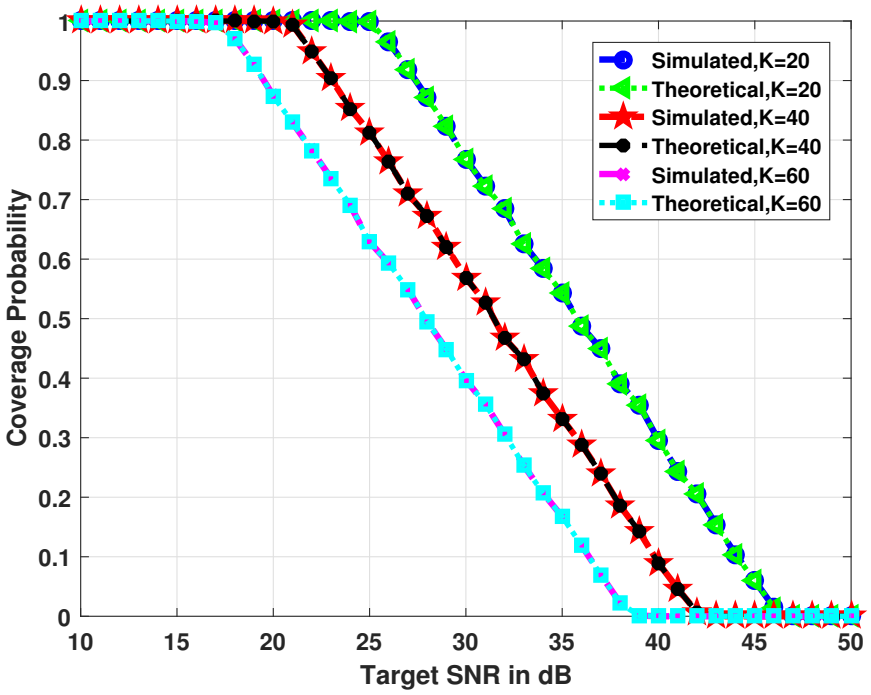

Figure 3.15. Average coverage probability for multi-user SIMO-PNC with $M = 100$ when the received SNR is uniformly distributed between 0 and 20 dB.

CHAPTER 4

NON-ORTHOGONAL MULTIPLE ACCESS BASED PHYSICAL LAYER NETWORK CODING

In this chapter, we propose a NOMA based MIMO-PNC system to increase further the spectral efficiency (Yılmaz et al., 2020). This chapter is organized as follows: First, the overview of related works are given. Then, the system model is represented. After, the proposed NOMA based MIMO-PNC is represented. Finally, performance evaluations are given.

4.1. Overview

NOMA is one of the key enabling multiple access technologies for 6G systems to fulfill the 6G requirements such as high data rate, ultra-low latency, large connectivity while enhancing the overall spectral efficiency. The main concept of NOMA is to simultaneously serve multiple users through the same time, same frequency or same code (Shi et al., 2020). In the literature, there are mainly two different type of NOMA technologies: Power-domain NOMA (S. M. R. Islam and Kwak, 2017) or code-domain NOMA (O. Shental and Shitz, 2017). In the power-domain NOMA (Wei et al., 2020), the power difference of the users is exploited for multi-user multiplexing while applying successive interference cancellation (SIC) or ML at the receivers to mitigate the inter-user interference .

In the literature, the latency performance of power-domain NOMA versus OMA has been also examined. Specifically, the work presented in (W. Yu and Ni, 2018) investigated the link layer capacity, namely, the effective capacity, of NOMA under probabilistic delay constraints and showed that NOMA outperforms OMA when the signal to noise ratio is high.

Despite the noticeable advantages of NOMA, other advanced technologies are also needed to achieve higher spectral efficiency. One of these technologies is MIMO. The

main idea of MIMO is to use multiple antennas at the BS to simultaneously serve many users by separating them in the spatial domain. Since MIMO provides extra degrees of freedom, the integration of NOMA and MIMO has recently become an attractive solution in terms of massive connectivity support (Shi et al., 2020). In the combined MIMO-NOMA scheme, users are divided into clusters which includes both near and far users. Then, the linear precoding schemes can be employed at the BS to suppress inter-cluster interference while SIC based detectors are applied at the user side to mitigate the intra-cluster users (Ali and Kim, 2016).

PNC is one of promising techniques for wireless communications to ensure network reliability for beyond fifth generation (B5G) systems (P. Chen and Rodrigues, 2016). In the literature, PNC has been combined with the NOMA without considering MIMO systems (Ho and Leow, 2019). In this thesis, we propose to combine the NOMA-MIMO systems with PNC to exchange information between UE pairs efficiently.

4.2. Proposed NOMA based MIMO-PNC

In this section, we give our proposed NOMA based MIMO-PNC. Our system given in Figure 4.1 consists of two sets which are the strong UEs and the weak UEs. Each set consists of $Q = K/2$ UEs. The SNR of the strong UEs is higher than the SNR of the weak users. These UEs communicate pairwise via the BS equipped with N antennas. We consider two scenarios for the pairing which is showed in Figure 4.2. For the first scenario, each strong UE is paired with a weak UE. For the second scenario, each weak UE is paired with a weak UE and each strong UE is paired with a strong UE. Thereby, all UEs modulate their QPSK modulation. We assume that BS have a perfect CSI, all UEs and BS are perfectly synchronized and all UEs transmit their signals simultaneously to the BS. For both two scenarios, the aim is to estimate NCS vector $\mathbf{x}_R \in \mathbb{C}^{Q\times 1}$. Let define the composite transmit symbol vector $\mathbf{x} \in \mathbb{C}^{K\times 1}$, which is obtained through the concatenation of the transmit symbols of the strong set $\mathbf{x}_1$ and weak set $\mathbf{x}_2$:

$$\mathbf{x} = \Big[\mathbf{x}_1, \mathbf{x}_2\Big]^T \tag{4.1}$$

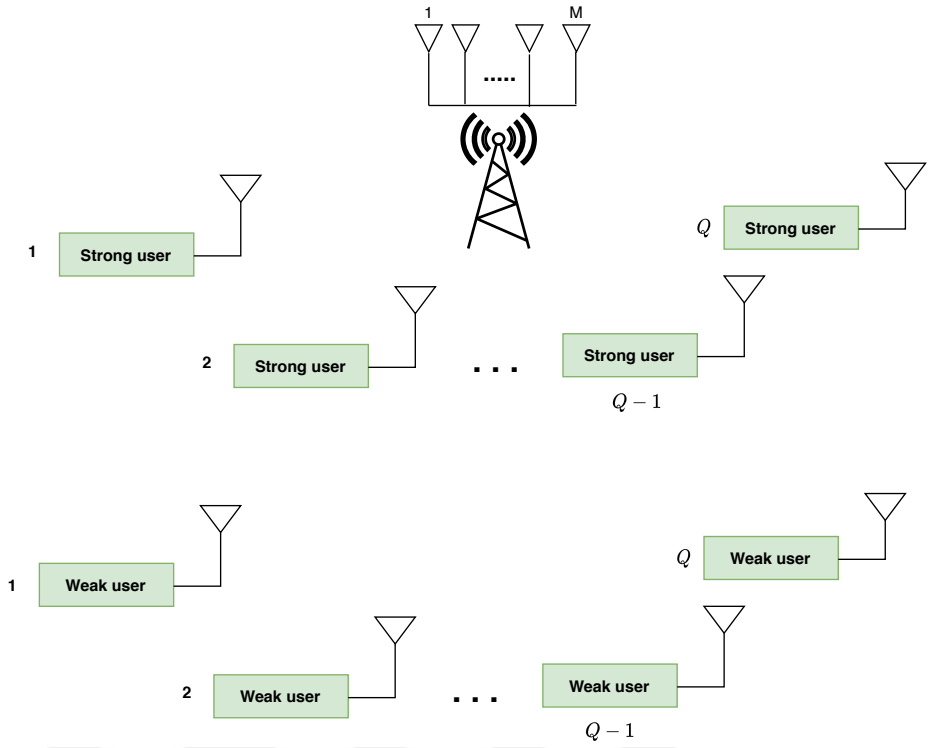

Figure 4.1. System Model for NOMA based MIMO-PNC

where

$$\mathbf{x}_1 = \left[x_{1,1}, x_{1,2}, \cdots, x_{1,Q}\right]^T \tag{4.2}$$

and

$$\mathbf{x}_2 = \left[x_{2,1}, x_{2,2}, \cdots, x_{2,Q}\right]^T \tag{4.3}$$

For the first scenario, where each strong UE is paired with a weak UE, the NCS vector is given as follows:

$$\mathbf{x}_R = \begin{bmatrix} x_{1,1} \oplus x_{2,1} \\ x_{1,2} \oplus x_{2,2} \\ \cdots \\ x_{1,Q} \oplus x_{2,Q} \end{bmatrix} \tag{4.4}$$

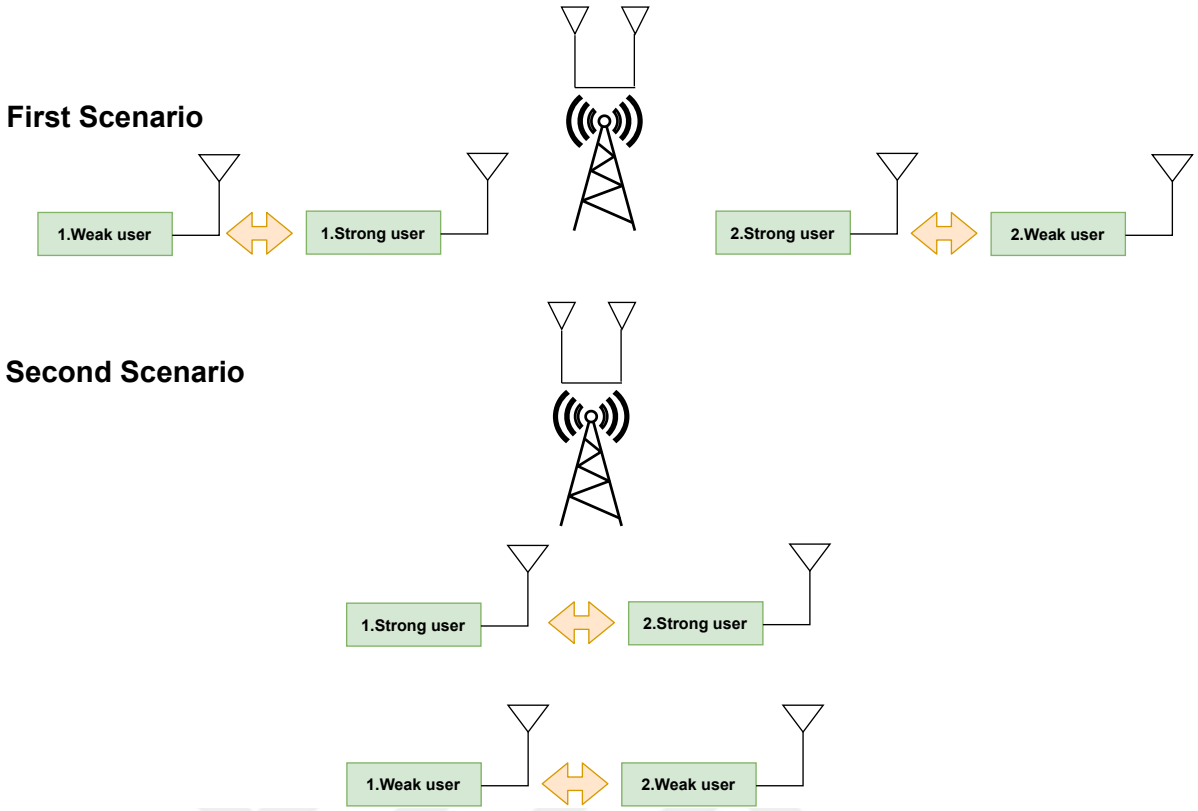

Figure 4.2. Pairing Scenarios for $M = 2, K = 4$

For the second scenario, where each strong UE is paired with a strong UE and each weak UE is paired with a weak UE, the NCS vector is given by the following equation:

$$\mathbf{x}_R = \begin{bmatrix} x_{1,1} \oplus x_{1,2} \\ x_{1,3} \oplus x_{1,4} \\ \cdots \\ x_{1,Q-1} \oplus x_{1,Q} \\ x_{2,1} \oplus x_{2,2} \\ x_{2,3} \oplus x_{2,4} \\ \cdots \\ x_{2,Q-1} \oplus x_{2,Q} \end{bmatrix} \tag{4.5}$$

The received vector $\mathbf{r} \in \mathbb{C}^{K \times 1}$ is given as follows:

$$\mathbf{r} = [\mathbf{H}_1, \mathbf{H}_2] \begin{bmatrix} \mathbf{x}_1 \\ \mathbf{x}_2 \end{bmatrix} + \mathbf{n} \tag{4.6}$$

where $\mathbf{H}_1, \mathbf{H}_2 \in \mathbb{C}^{M \times Q}$ are the composite channel matrices of strong and weak sets whose elements are the complex Gaussian random variables which have zero means and unity variances and $\mathbf{x}_1 \in \mathbb{C}^{Q \times 1}$ and $\mathbf{x}_2 \in \mathbb{C}^{Q \times 1}$ are the transmit symbol vectors for the strong and weak sets respectively which are given in Eq.(4.1). $\mathbf{H} = [\mathbf{H}_1, \mathbf{H}_2]$ is the composite channel matrix with the dimension of $M \times K$ which is obtained by the composition of $\mathbf{H}_1$ and $\mathbf{H}_2$. Then, the received vector can be arranged as:

$$\mathbf{r} = \mathbf{H}\mathbf{x} + \mathbf{n} = (\mathbf{H}\mathbf{D}^{-1})(\mathbf{D}\mathbf{x}) + \mathbf{n} = \hat{\mathbf{H}}\hat{\mathbf{x}} + \mathbf{n} \tag{4.7}$$

where the manipulated composite channel matrix $\hat{\mathbf{H}} \in \mathbb{C}^{M \times K}$ is given as $\hat{\mathbf{H}} = \mathbf{H}\mathbf{D}^{-1}$. For the first pairing scenario, the sum difference matrix $\mathbf{D} \in \mathbb{C}^{K \times K}$ is given in Eq.(2.49). Then, the target estimated vector $\hat{\mathbf{x}} = \mathbf{D}\mathbf{x}$ whose elements are sum and differences of the paired transmit symbols is given by the following equation:

$$\hat{\mathbf{x}} = \begin{bmatrix} x_1 + x_{Q+1} \\ x_2 + x_{Q+2} \\ \cdots \\ x_Q + x_{2Q} \\ x_1 - x_{Q+1} \\ x_2 - x_{Q+2} \\ \cdots \\ x_Q - x_{2Q} \end{bmatrix} \tag{4.8}$$

For the second pairing scenario, we propose to use the following the sum difference matrix:

$$\mathbf{D} = \begin{bmatrix} \mathbf{D}_{2\times 2} & 0 & 0 \\ 0 & \mathbf{D}_{2\times 2} & 0 \\ 0 & 0 & \mathbf{D}_{2\times 2} \end{bmatrix} \tag{4.9}$$

where $\mathbf{D}_{2\times 2}$ is the smallest sum-difference matrix. Then, the target estimated vector $\hat{\mathbf{x}} = \mathbf{D}\mathbf{x}$, is given as follows:

$$\hat{\mathbf{x}} = \begin{bmatrix} x_1 + x_2 \\ x_1 - x_2 \\ x_3 + x_4 \\ x_3 - x_4 \\ \cdots \\ x_{2Q-1} + x_{2Q} \\ x_{2Q-1} - x_{2Q} \end{bmatrix} \tag{4.10}$$

Then, BS equalizes the received vector by the following equation:

$$\mathbf{y} = \mathbf{W}\mathbf{r} \tag{4.11}$$

where $\mathbf{W} \in \mathbb{C}^{K\times M}$ and $\mathbf{y} \in \mathbb{C}^{K\times 1}$ are the equalization matrix and equalized vector respectively. For ZF solution, the equalization matrix $\mathbf{W}$ is given as follows:

$$\mathbf{W} = (\hat{\mathbf{H}})^{\dagger} = (\hat{\mathbf{H}}^H\hat{\mathbf{H}})^{-1}\hat{\mathbf{H}}^H \tag{4.12}$$

For MMSE solution, the equalization matrix $\mathbf{W}$ is given in Eq.(2.89) for the users having different SNR values. Then, LLR value of each symbol pair is defined in Eq.(2.73). Finally, according to the LLR value, BS decides on the NCS value of each symbol pair and form NCS vector according to the rule given in Eq.(2.88).

4.3. Performance Evaluations

In this section, the CDF of BER for NOMA based MIMO-PNC is given when UEs modulate their data with QPSK modulation. As a linear detection technique, ZF and MMSE are used to provide simulation results. For all simulation results SNR value of each strong user is set to 30dB and the SNR value of each weak user is set 10dB. According to the results, the applicability of the PNC in the NOMA based MIMO systems has been demonstrated efficiently. Besides, it is observed that the strong-strong and the weak-weak pairing outperforms the strong-weak pairing. Further, it is showed that MMSE has a better performance rather than ZF for NOMA based MIMO-PNC. Finally, it is demonstrated that NOMA based PNC outperforms NOMA based MIMO-NC for strong-weak pairing and for linear detectors.

In the Figures 4.3 and 4.4, it is plotted the CDF of BER for NOMA based MIMO-PNC with ZF and MMSE for strong-weak pairing and strong-strong and weak-weak pairing with $M = 2$, $K = 4$ and $M = 4$, $K = 8$ respectively for QPSK modulation. For these two figures, it is concluded that the strong-strong,weak-weak pairing outperforms the strong-weak pairing. Further, it is also demonstrated that the performance of the MMSE is better than ZF for both two cases. Then, it is showed that when the number of user is increased the performance of the system degrades.

In the Figure 4.6, it is provided the CDF of BER for NOMA based MIMO-PNC and NOMA based MIMO-NC with ZF and MMSE for strong-weak pairing with $M = 2$, $K = 4$ for QPSK modulation. Thereby, it is observed that NOMA based MIMO-PNC outperforms NOMA based MIMO-NC for linear detectors.

In the Figure 4.5, it is plotted the CDF of BER for NOMA based MIMO-PNC with ZF and MMSE for both two pairing scenarios when the SNR values of the weak users are uniformly distributed between 5 and 15dB and SNR values of the strong users are uniformly distributed between 25 and 35dB with $M = 2$, $K = 4$ for QPSK modulation. It is observed that, for a more realistic scenario, when the SNR values of two sets are uniformly distributed within some ranges, NOMA is still applicable in MIMO-PNC systems.

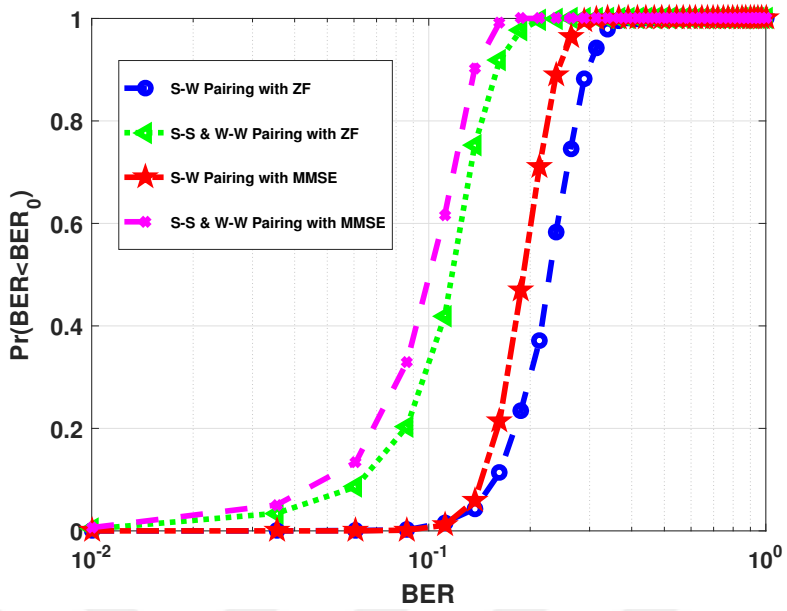

Figure 4.3. CDF of BER for NOMA based MIMO-PNC with ZF and MMSE for strong-weak pairing and strong-strong and weak-weak pairing, $M = 2$, $K = 4$, SNR of weak users: 10dB, SNR of strong users: 30dB, for QPSK

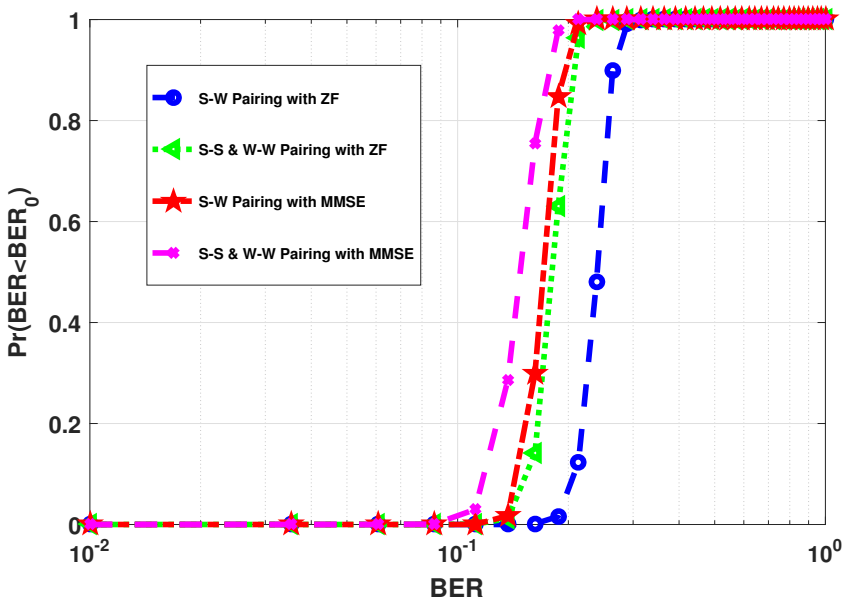

Figure 4.4. CDF of BER for NOMA based MIMO-PNC with ZF and MMSE for strong-weak pairing and strong-strong and weak-weak pairing, $M = 4$, $K = 8$, SNR of weak users: 10dB, SNR of strong users: 30dB, for QPSK

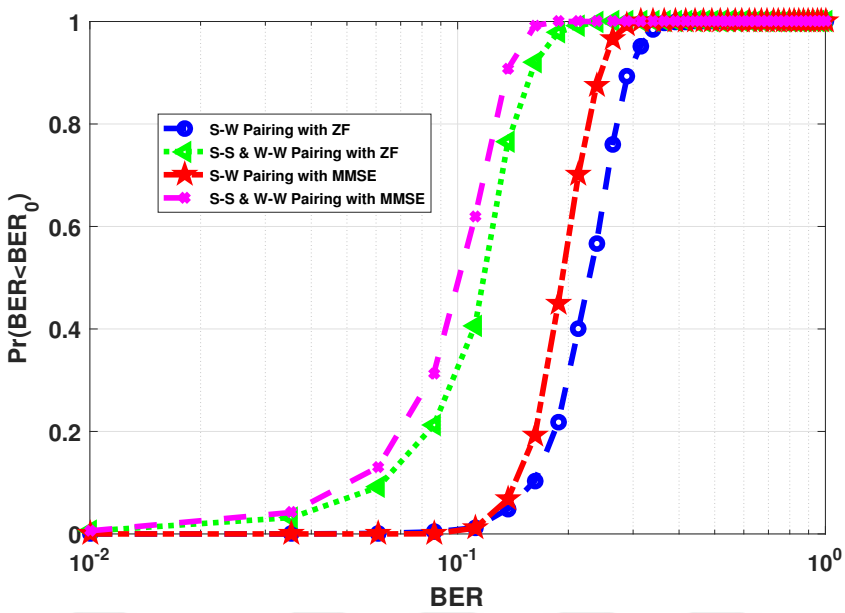

Figure 4.5. CDF of BER for NOMA based MIMO-PNC with ZF and MMSE for strong-weak pairing and strong-strong and weak-weak pairing, $M = 2$, $K = 4$, SNR value of weak users is uniformly distributed between 5 and 15dB, SNR values of strong users are uniformly distributed between 25 35dB, for QPSK

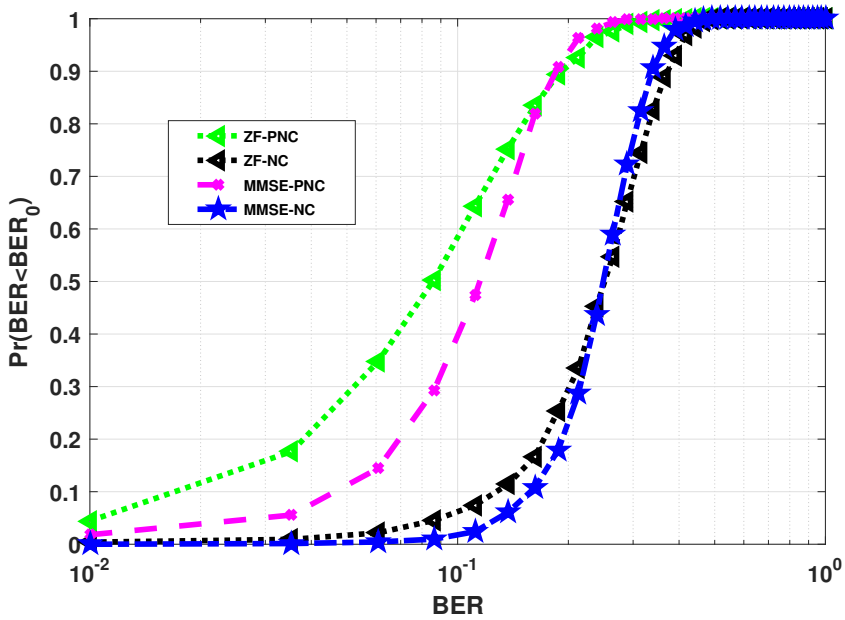

Figure 4.6. CDF of BER for NOMA based MIMO-PNC and MIMO-NC with ZF and MMSE for strong-weak pairing, $M = 2$, $K = 4$, SNR of weak users: 10dB, SNR of strong users: 30dB, for QPSK

CHAPTER 5

CONCLUSION

In this thesis, PNC has been examined based BER and coverage probability in single antenna systems, MIMO systems, multi-user massive MIMO systems and NOMA systems.

In the single antenna systems, the theoretical and simulation BER performance of the PNC, NC and BPSK has been provided. PNC has a better performance compared with the NC. For MIMO systems, the performance gain of the PNC on NC has become significant. For the multi-user massive MIMO systems, we conclude that PNC outperforms NC in the higher SNR regime. When the users have different SNR value as the difference increases, the performance of PNC and NC converges. Since the previous detection scheme for MIMO-PNC uses LLR, it has come with a complexity. We propose a low complex technique which has a slight gain on MIMO-NC.

Then, the coverage analysis has been made for PNC. The conventional SNR distribution definitions have been adapted to the MIMO-PNC scheme. Then, the closed form coverage probability expression has been proposed. First, it is observed that our theoretical results are perfectly matched with the simulation results. Then, it is also observed that even the target SNR is greater than the average received SNR, BS can cover the users by 100 percent due to the performance boosting properties of both PNC and MIMO. For fixed number of the users in the network, as the antenna number in the BS increases, the coverage probability is also increased. On the other hand, for fixed number of the antennas at the BS, as the number of user increases, the BS can cover less users. A transition region is observed while the target SNR increases. BS's coverage probability decreases within this transition region. When the received SNR is randomly distributed, the width of this transition region is greater than the case for fixed received SNR.

Finally, we give our proposed NOMA based MIMO-PNC. As the performance evaluations, we give the CDF of BER for NOMA based MIMO-PNC system for two different pairing scenarios and for linear detectors. We conclude that NOMA based MIMO-PNC with MMSE detector outperforms NOMA based MIMO-PNC with ZF. Then, it is

observed that strong-strong and weak-weak pairing scenario outperforms the strong-weak pairing scenario. We compare also NOMA based MIMO-PNC and NOMA based MIMO-NC for strong-weak pairing scenario. It is concluded that NOMA based MIMO-PNC outperforms NOMA based MIMO-NC for ZF and MMSE detectors when the strong-weak pairing scenario is considered.

As the future works, the proposed coverage analysis can be extended to the multi-cell massive MIMO-PNC in unsupervised networks. Further, proposed NOMA based MIMO-PNC can be examined for internet of things (IoT) applications.

REFERENCES

Shental, Ori, Benjamin Zaidel and Shlomo Shitz (2017). Low-density code-domain NOMA: Better be regular. In *IEEE International Symposium on Information Theory (ISIT)*, Aachen,Germany, pp. 2628–2632.

Albreem, Mahmoud, Markku Juntti and Shahriar Shahabuddin (2019). Massive MIMO Detection Techniques: A Survey. *IEEE Communications Surveys Tutorials 21*(4), 3109–3132.

Ali, Shipon, Ekram Hossain and Dong In Kim (2016). Non-orthogonal multiple access (NOMA) for downlink multiuser MIMO systems: User clustering, beamforming, and power allocation. *IEEE access 5*, 565–577.

Andrews, Jeffrey, Abhishek Gupta and Harpreet Dhillon (2016). A primer on cellular network analysis using stochastic geometry. *CoRR abs/1604.03183*.

Chen, Pingping, Zhaopeng Xie, Yi Fang, Zhifeng Chen, Shahid Mumtaz and Jonathan Rodrigues (March/April, 2016). Physical-layer network coding: An efficient technique for wireless communications. *IEEE Network 34*(2), 270–276.

Chu, Eunmi, Jae Sook Yoo and Bang Chul Jung (Jul. 2017). Spatial-modulated physical-layer network coding in two-way relay networks with convolutional codes. In *Ninth International Conference on Ubiquitous and Future Networks (ICUFN)*, Milan,Italy, pp. 811–813.

Fang, Dong (2014). *Physical-layer Network Coding for Cooperative Wireless Networks*. Ph. D. thesis, University of York.

Fukui, Hironori, Petar Popovski and Hiroyuki Yomo (Nov. 2014). Physical layer network coding: An outage analysis in cellular network. In *22nd European Signal Processing Conference (EUSIPCO)*, Lisbon,Portugal, pp. 1133–1137.

Gore, Dhananjay, Robert Heath and Arogyaswami Paulraj (2002). On performance of the zero forcing receiver in presence of transmit correlation. In *Proceedings IEEE International Symposium on Information Theory*, Lausanne, pp. 159.

Ho, Chun Yeen and Chee Yen Leow (2019). Cooperative non-orthogonal multiple access with physical layer network coding. *IEEE Access 7*, 44894–44902.

İlgüy, Mert, Berna Özbek, Shahid Mumtaz, Sherif Busari and Jonathan Gonzalez (2020). Coverage Analysis of Physical Layer Network Coding in Massive MIMO Systems. Major revision in IEEE Transactions on Vehicular Technology.

Islam, Sayeed, Nurilla Avazov, Octavia Dobre and Kyung-sup Kwak (2017). Power-Domain Non-Orthogonal Multiple Access (NOMA) in 5G Systems: Potentials and Challenges. *IEEE Communications Surveys and Tutorials 19*(2), 721–742.

Kay, Steven (1993). *Fundamentals of statistical signal processing*. Prentice Hall PTR.

Khoshkholgh, Mohammad, Keivan Navaie, Kang Shin and Victor Leung (Dec. 2017). Coverage Analysis of Multi-Stream MIMO HetNets With MRC Receivers. *16*(12), 7816–7833.

Kumar, Suman, Sheetal Kalyani, Lajos Hanzo and Krishnamurthy Giridhar (Oct. 2015). Coverage Probability and Achievable Rate Analysis of FFR-Aided Multi-User OFDM-Based MIMO and SIMO Systems. *IEEE Transactions on Communications 63*(10), 3869–3881.

Kumar, Vahibhav, Barry Cardiff and Mark Flanagan (May. 2019). User-antenna selection for physical-layer network coding based on euclidean distance. *IEEE Transactions on Communications 67*(5), 3363–3375.

Li, Yiping, Shengli Zhang and Hui Wang (Aug. 2013). BER performance analysis of MIMO Physical-layer Network Coding based on VBLAST detection. In *IEEE/CIC International Conference on Communications in China-Workshops (CIC/ICCC)*,

Xian,China, pp. 170–175.

Loan, Charles and Gene Golub (1983). *Matrix Computations* (Third ed.). Baltimore, Maryland: The Johns Hopkins University Press.

Louie, Raymond, Younghui Li and Branka Vucetic (Nov. 2009). Performance analysis of physical layer network coding in two-way relay channels. In *GLOBECOM IEEE Global Telecommunications Conference*, Honolulu, HI, USA, pp. 1–6.

Lu, Kejie, Shengli Fu, Yi Qian and Hsiao-Hwa Chen (Nov. 2009). SER Performance Analysis for Physical Layer Network Coding over AWGN Channels. In *GLOBECOM IEEE Global Telecommunications Conference*, Honolulu,HI,USA, pp. 1–6.

Lu, Mingyue, Shenand Zhongliang, Daoxing Guo and Xi Wang (Jun. 2017). A new physical layer network coding de-noising mapping based on M-QAM. In *First International Conference on Electronics Instrumentation and Information Systems (EIIS)*, Harbin,China, pp. 1–5.

Monhof, Stefan, Stefan Bocker, Janis Tiemann and Christian Wietfeld (Oct. 2018). Cellular network coverage analysis and optimization in challenging smart grid environments. In *IEEE International Conference on Communications, Control, and Computing Technologies for Smart Grids (SmartGridComm)*, Aalborg, Denmark, pp. 1–6.

Namboodiri, Vishnu, Kiran Venugopal and Balaji Sundar Rajan (Oct. 2013). Physical Layer Network Coding for Two-Way Relaying with QAM. *IEEE Transactions on Wireless Communications 12*(10), 5074–5086.

Okyere, Bismark, Leila Musavian and Shahid Mumtaz (Dec. 2019). Multi-User Massive MIMO and Physical Layer Network Coding. In *IEEE Globecom Workshops (GC Wkshps)*, Waikoloa, HI, USA, pp. 1–6.

Panziyu, Yangjie and Huhan Baoziyong (Oct. 2018). Approximate coverage analysis of

heterogeneous cellular networks modeled by poisson hole process. In *IEEE 18th International Conference on Communication Technology (ICCT)*, Chongqing, China, pp. 424–427.

Parida, Priyabrata and Harpreet Dhillon (Mar. 2019). Stochastic Geometry-Based Uplink Analysis of Massive MIMO Systems With Fractional Pilot Reuse. *IEEE Transactions on Wireless Communications 18*(3), 1651–1668.

Razeghi, Behrooz, Ghosheh Abed Hodtani and Seyen Alireza Seyedin (Sep. ,2014). Coverage region analysis for MIMO amplify-and-forward relay channel with the source to destination link. In *7'th International Symposium on Telecommunications*, Tehran,Iran, pp. 1133–1137.

Renzo, Marco Di and Peng Guan (Aug. 2014). A Mathematical Framework to the Computation of the Error Probability of Downlink MIMO Cellular Networks by Using Stochastic Geometry. *IEEE Transactions on Communications 62*(8), 2860–2879.

Shi, Zheng, Hong Wang, Yaru Fu, Guanghua Yang, Shaodan Ma, Fen Hou and Theodoros Tsiftsis (2020). Zero Forcing Based Downlink Virtual MIMO NOMA Communications in IoT Networks. *IEEE Internet of Things Journal 7*(4), 2716–2737.

Sykora, Jan and Alister Burr (2018). *Wireless Physical Layer Network Coding*. Cambridge University Press.

Wei, Zhiqiang, Lei Yang, Derrick Wing Kwan Ng, Jinhong Huan and Lajos Hanzo (2020). On the Performance Gain of NOMA Over OMA in Uplink Communication Systems. *IEEE Transactions on Communications 68*(1), 536–568.

Yılmaz, Simay, Berna Özbek, Mert İlgüy, Bismark Okyere and Leila Musavian (2020). User Selection for NOMA based MIMO with Physical Layer Network Coding in Internet of Things Applications. Major revision in IEEE Internet of Things Journal.

Yu, Wenjuan, Leila Musavian and Qiang Ni (Oct. 2018). Link-Layer Capacity of NOMA Under Statistical Delay QoS Guarantees. *IEEE Transactions on Communications 66*(10), 4907–4922.

Zhang, Shengli and Soung Liew (Apr. 2010). Physical layer network coding with multiple antennas. In *IEEE Wireless Communication and Networking Conference*, Sydney,Australia, pp. 1–6.

Zhang, Shengli, Soung Liew and Patrick Lam (2006). Hot topic: Physical-layer network coding. In *Proceedings of the 12th annual international conference on Mobile computing and networking*, pp. 358–365.